World Scientific
www.worldscientific.com

JAPAN SOCIETY OF CIVIL ENGINEERS
COASTAL ENGINEERING COMMITTEE

Coastal Engineering Journal, Vol. 52, No. 1 (2010) 71–106

DOI: 10.1142/S0578563410002129

REANALYSIS OF REGULAR AND RANDOM BREAKING WAVE STATISTICS*

YOSHIMI GODA
Professor Emeritus at Yokohama National University,
ECOH CORPORATION, 2-6-4 Kita-Ueno,
Taito-Ku, Tokyo 110-0014, Japan
goda@ecoh.co.jp

Received 16 November 2007
Revised 5 January 2010

Statistics of breaking waves across the surf zone are reanalyzed on the basis of various sets of field and laboratory data so as to provide coastal engineers with reliable information on breaking waves. The breaker index or the ratio of wave height to water depth is to be expressed as a function of the two parameters of beach slope and relative depth, and Goda's breaker index formula is revised slightly to reduce the slope effect. The breaker index for regular waves has inherent variability as expressed with the coefficient of variability, which increases from 6% to 14% as the beach slope becomes steep up to 1/10. The incipient breaking height of the significant wave is about 30% lower than that of regular waves, but the ratio of significant wave height to water depth gradually increases within the surf zone toward the shoreline. The wave height distribution is the narrowest in the middle of the surf zone, but it returns to the Rayleigh distribution near the shoreline owing to wave regeneration after breaking. The nonlinearity of random waves is strongest at the outer edge of the surf zone, but it is destroyed by the wave breaking process inside the surf zone. The ratios of statistical wave heights $H_{1/10}$, $H_{1/3}$ and $H_{\rm rms}$ to the spectral significant wave height H_{m0} are shown to increase as the wave nonlinearity parameter increases up to the outer edge of the surf zone.

Keywords: Wave breaking; breaker index; wave height ratio; characteristic wave heights; spectral significant wave height; skewness; kurtosis; nonlinearity parameter; irregular waves.

*The present paper is an expanded version of the author's paper presented at the 54th Japanese Coastal Engineering Conference in November 2007. The Japanese paper was awarded as one of the best three papers at the conference by the Coastal Engineering Committee of the Japan Society of Civil Engineers.

Notations

The following symbols are used in this paper:

A = proportionality coefficient of breaker index formula;
H_0 = deepwater wave height;
H_0' = equivalent deepwater wave height;
$H_{1/3}$ = one-third highest wave height defined by zero-crossing method, or statistical significant wave height;
$H_{1/10}$ = one-tenth highest wave height defined by zero-crossing method;
H_b = regular wave height at breaking;
H_{m0} = energy-based significant wave height defined by Eq. (9);
$H_{\rm rms}$ = root-mean-square wave height defined by zero-crossing method;
h = water depth;
h_b = water depth at breaking of regular waves;
L_0 = deepwater wavelength of small amplitude waves;
L_A = wavelength of small amplitude waves in arbitrary depth;
$(L_F)_0$ = deepwater wavelength of finite amplitude waves;
m_0 = zero-th moment of frequency spectrum;
s = beach slope;
T = wave period;
$T_{1/3}$ = significant wave period defined by zero-crossing method;
β_1 = skewness defined by Eq. (12);
β_2 = kurtosis defined by Eq. (13);
$\beta_{\rm rms}$ = root-mean-square value of surface elevation;
Π_0 = wave nonlinearity parameter defined by Eq. (16);
$\Pi_{1/3}$ = wave nonlinearity parameter defined by Eq. (14);
θ_0 = deepwater incident wave angle.

1. Introduction

Breaking of water waves is the most important element in coastal engineering design. It exerts the largest wave actions on structures against which the structures have to maintain their integrity. Wave breaking induces the nearshore currents which carry sediment in suspension and cause beach deformation. Nonetheless, quantitative examination of wave breaking statistics is rather inadequate. Many engineers and researchers seem to have a few mistaken concepts on wave breaking. First, the ratio of wave height to water depth at breaking, $(H/h)_b$, which is called the breaker index, is thought to be a fixed value, such as 0.78. Second, the breaker index of the significant wave is often regarded as the same as that for regular waves. Both concepts are incorrect and will be discussed in the present paper.

The study on breaking waves dates back to McCowan [1894], who calculated the limiting height H of solitary wave being 0.78 times the water depth h. Munk [1949]

used this ratio as the breaker height of solitary wave for engineering applications. McCowan's result has been revised by Yamada *et al.* [1968] with a more accurate value of 0.8261, but only a few people are aware of the improvement achieved by them.

The limit of the steepness of deepwater waves was calculated by Miche [1944] as $H_0/(L_F)_0 = 0.142$, and Yamada and Shiotani [1968] presented a revised value of $H_0/(L_F)_0 = 0.1412$. Many people have referred to Miche's value of 0.142, but they have often overlooked the definition of deepwater wavelength $(L_F)_0$ by Miche, which is the length of finite amplitude waves. According to the calculation by Yamada and Shiotani, the wavelength of permanent waves at the breaking limit is 119.3% of the small amplitude wavelength $L_0 = (g/2\pi)T^2$, where g is the gravitational acceleration and T is the wave period. When the small amplitude wavelength L_0 is employed instead of the finite amplitude wavelength $(L_F)_0$, the breaking limit of deepwater waves is expressed as $(H_0/L_0)_b = 0.1684$.

The present paper aims at providing the readers with as many data as possible on the phenomenon of regular and random wave breaking and clarifying the ambiguity related with wave breaking process. The paper first examines the breaker index of regular waves on the basis of various laboratory data available. The breaker index is shown to be governed by the two parameters of beach slope s and relative depth h/L. Laboratory data also demonstrate that the breaker index is characterized with an inherent variability, which amount to about 6% to 14% depending to the bottom slope.

Next, the breaker index of irregular waves is reviewed for the incipient breaking stage at the outer edge of the surf zone and the developed breaking stage inside the surf zone.

Third, evolution of the probability density function of individual wave heights across the surf zone is discussed. In the offshore, individual wave heights almost follow the Rayleigh distribution. However, the wave height distribution in the surf zone becomes narrower than the Rayleigh, and the differences between characteristic wave heights such as $H_{2\%}$, $H_{1/10}$, $H_{1/3}$ and $H_{\rm rms}$ decrease toward the middle of the surf zone. Then, the trend of decrease is reversed with the increase of wave height ratios as waves come near to the shoreline.

Fourth, evolution of wave nonlinearity across the surf zone is surveyed in terms of the skewness and kurtosis of surface elevation and the ratios of statistical wave heights such as $H_{1/10}$, $H_{1/3}$, and $H_{\rm rms}$ to the spectral significant wave height H_{m0}. Several databases of field wave measurements are employed for analysis.

2. Breaker Index Formula and Variability

2.1. *Previous studies on breaking wave statistics*

The earliest laboratory data on wave breaking was provided by Iversen [1951], who presented four tables and diagrams of breaking wave statistics on the beach slopes

Table 1. Summary of breaker index data sets of regular waves.

Author	Beach slope	Wave period T (s)	Breaking wave Height H_b (cm)	Breaking depth hb (cm)	Nos. data	Wave flume L×D×B (m)
Iversen [1951]	1/10	0.80–2.50	4.9–12.2	4.3–13.7	15	16.4×0.9×0.3
	1/20	0.74–2.24	4.3–12.8	4.9–16.2	19	
	1/30	1.49–2.65	5.3–12.7	7.0–15.5	15	
	1/50	0.90–2.65	5.5–12.1	6.5–15.6		
Kishi and Iohara [1958]	1/9	0.9–2.0	7.0–10.6	7.9–10.0	4	13.0×0.5×0.6
	1/17	0.65–2.0	5.0–12.5	6.5–13.5	21	
Mitsuyasu [1962]	1/15	1.02–2.57	10.4–15.0	12.4–14.5	4	22.0×0.5×0.6
	1/30	1.02–2.57	9.6–11.1	15.3–20.6	4	
	1/50	1.02–2.57	9.8–14.1	17.7–19.0	4	
Goda [1964]	1/100	2.30–7.30	41.7–93.1	60.3–125.0	32	105.0×2.5×3.0
Goda *et al.* [1966]	1/10	1.36–2.24	14.0–21.5	11.0–18.0	6	33.1×0.9×0.5
Toyoshima *et al.* [1968]	1/20	1.84–3.04	6.2–40.8	7.3–61.0	22	112.0×2.5×1.5
	1/30	1.94–3.75	11.9–50.0	13.1–61.6	44	
Bowen *et al.* [1968]	1/12	0.82–2.27	4.4–13.0	4.2–9.7	11	40.0×0.75×0.5
Galvin [1969]	1/10	1.00–6.00	3.8–15.0	3.9–12.0	8	29.3×0.6×0.46
	1/20	2.00–6.00	9.3–17.6	10.0–18.2	6	
Li *et al.* [1991]	1/30	—	—	—	10	69.0×2.0×2.0
	1/50				11	
Li *et al.* [2000a]	1/200	—	—	—	19	69.0×2.0×2.0
Lara *et al.* [2006]	1/20	1.20–4.00	6.7–18.5	6.8–19.5	12	24.0×0.8×0.6

of 1/10, 1/20, 1/30, and 1/50. Then, several datasets on breaking wave statistics have become available as listed in Table 1, although there would have been many more datasets which were not readily available to the present author. Breaking of regular waves is easily recognized by an experimentalist and the data of breaking wave height and depth reported by each researcher are listed here.

By using the datasets available at the time, Goda [1970] prepared the diagrams of breaker index for four beach slopes of 1/10, 1/20, 1/30, and 1/100 by referring to the theoretical limiting wave heights on the horizontal bed calculated by Yamada and Shiotani [1968]; their calculation results have been reproduced as Table B6.1 of ISO [2007] and in Goda [2007]. Then, Goda [1973, 1974] converted the graphical curves of breaker index into a functional form of the following for the convenience of wave pressure computation of composite breakwaters:

$$\frac{H_b}{h_b} = \frac{A}{h_b/L_0}\left\{1 - \exp\left[-1.5\pi\frac{h_b}{L_0}(1 + 15s^{4/3})\right]\right\} : A = 0.17 \tag{1}$$

Coastal engineers in Japan have been using this formula in routine design works, but it is not as widely known in the United Sates. Nevertheless, the formula is listed in the Rock Manual [CIRIA *et al.*, 2007].

Studies on breaking wave statistics have continued through the 1970s to 1990s. Rattanapikikon and Shibayama [2000] list 24 formulas for estimating breaker heights, and Rattanapitikon *et al.* [2003] add five more formulas for the examination of their performances. The latter has analyzed 574 data points in small-scale wave flumes and 121 data points in large-scale flumes, though the data of Goda [1964] in Table 1 were not included.

2.2. *Parameters of breaker index formula*

The term of breaker index may include several definitions of wave height ratios such as H_b/h_b, H_b/H_0', h_b/H_0', etc., where H_0' denotes the equivalent deepwater wave height (see Goda [2009] for the definition of the equivalent deepwater wave height). Kaminsky and Kraus [1993] have proposed to use the exact terminology of the breaker-height-to-depth index, but the present paper employs the term of breaker index for the ratio of H_b/h_b for the sake of simplicity. The other breaker ratios of H_b/H_0' and h_b/H_0' can identify the breaking condition of *regular waves*, but they are not workable for *irregular waves*, which undergo transformation and breaking over a wide distance and there is no unique breaking point. Unless some definitions are given for the representative height and depth of random breaking waves, the breaker ratios of H_b/H_0' and h_b/H_0' are not usable in engineering practice for random waves; they are not discussed in the present paper.

By referring to the types of the breaker index formulas analyzed by Kamphuis [1991], their functional forms can be classified into the following four types:

$$H_b/h_b = f_1(0) = \text{constant} \tag{2}$$

$$H_b/h_b = f_2(h_b/L_0 \text{ or } h_b/L_b) \tag{3}$$

$$H_b/h_b = f_3(s) \tag{4}$$

$$H_b/h_b = f_4(s, h_b/L_0 \text{ or } h_b/L_b) \tag{5}$$

Because the relative water depth h_b/L_0 is easily converted to h_b/L_b through the dispersion relationship, the two relative depths h_b/L_0 and h_b/L_b are interchangeable; the former is mainly used in the present paper. The formula of $H_b/h_b = 0.78$ is a typical example of Eq. (2). There are some other formulas using the parameter of deepwater wave steepness H_0/L_0, but they are introduced mostly to estimate the ratios H_b/H_0' and h_b/H_0', which are not employed in random wave analysis, as discussed before.

Performance of a breaker index formula can be judged by the magnitude of the bias of the predicted breaker height from the observed heights. It should also be examined with either the root-mean-square error of predicted breaker heights

or the correlation coefficient between prediction and observation. The root-mean-square error analysis by Rattanapitikon and Shibayama [2000] is not conclusive in differentiating the merits of four functional forms, but they recommend a certain modifications of the slope effect in the function $f_4(s, h_b/L_0)$, apparently indicating their preference of this functional form.

Kamphuis [1991] calculated the correlation coefficients between eleven formulas and his laboratory data. By assigning the best-fitting value to the proportionality coefficient of each formula, he obtained the correlation coefficient $R^2 = 0.69$ to $f_1(0)$, $R^2 = 0.67$ to $f_2(h_b/L_0)$, $R^2 = 0.84$ to $f_3(s)$, and $R^2 = 0.88$ to $f_4(s, h_b/L_0)$. His result clearly suggests the necessity to include both the parameters of beach slope and relative water depth in the breaker index formula.

2.3. *New breaker index of regular waves*

The breaker index formula of Eq. (1) was derived by a graphical curve-fitting technique without direct comparison with the original laboratory data. Rattanapitikon and Shibayama [2000] have recommended a modification of the slope effect term of $(1 + 15s^{4/3})$ into $(1.033 + 4.71s - 10.46s^2)$. Upon re-examination of the original laboratory data, the present author has also recognized a necessity of modifying the slope effect term. The revision is made to replace the slope effect term with $(1 + 11s^{4/3})$ as in the following:

$$\frac{H_b}{h_b} = \frac{A}{h_b/L_0}\left\{1 - \exp\left[-1.5\pi\frac{h_b}{L_0}(1 + 11s^{4/3})\right]\right\} : A = 0.17 \tag{6}$$

Equation (6) yields a reduction of 11% of the breaker height on the beach slope of $s = 1/10$, but the reduction is only 2% for the beach slope of $s = 1/50$.

Muttray and Oumeraci [2000] found the best-fitting coefficient of Eq. (1) being 0.167 instead of 0.170 for the slope of 1/30. When Eq. (6) is applied to their data, the coefficient would have the value of 0.173.

Comparison of the laboratory data of breaker index with Eq. (6) is shown in Fig. 1 for six groups of beach slopes, i.e. 1/9 to 1/12, 1/20, 1/30, 1/50, 1/100 to 1/200, and zero inclination. A summary of the characteristics of datasets has been listed in Table 1. The data of beach slopes of 1/15 by Mitsuyasu [1962] and 1/17 by Kishi and Iohara [1958] are not plotted in Fig. 1 to avoid confusion because they belong to the slopes in between 1/10 and 1/20. Figure 1 includes the zero slope data that were obtained through the experiment by Danel [1951]. According to Hamm [1995], Danel employed a special wave flume, the width of which was gradually narrowing toward the spending beach. Thus, waves over a horizontal bed were forced to break at some location of the wave flume owing to gradual concentration of wave energy in a narrowed section. The wavelength was measured *in situ* so that it represented the finite amplitude wavelength. Hamm [1995] converted it into the small amplitude wavelength and he kindly provided the author with the data file: Danel's dataset consisted of 46 data points.

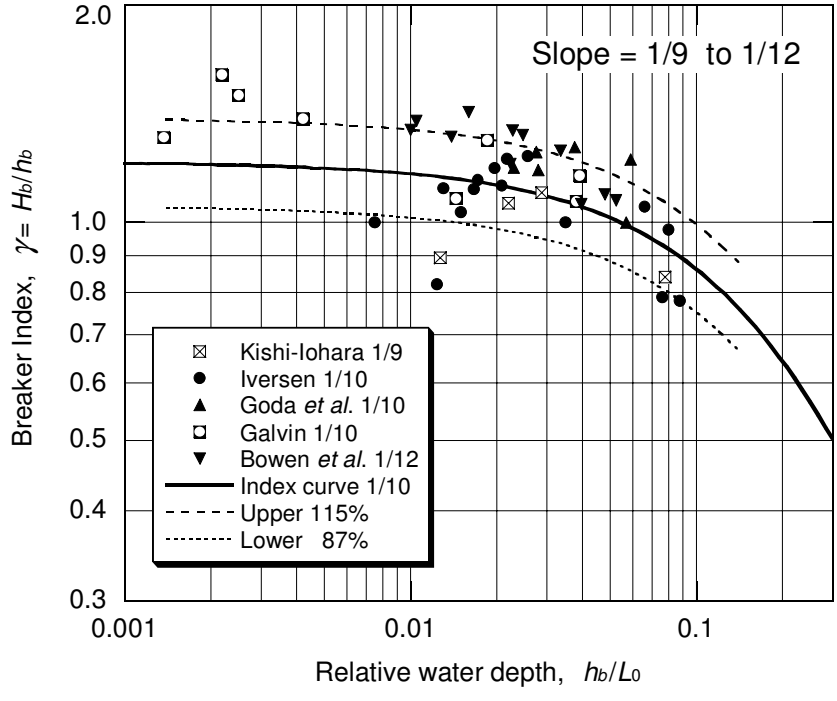

(a)

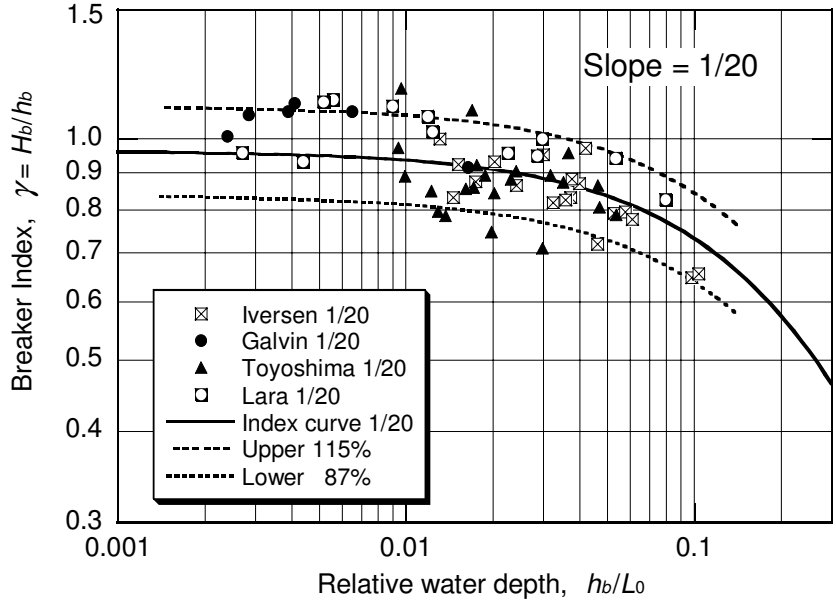

(b)

Fig. 1. Comparison of the new breaker index formula Eq. (6) with laboratory data of regular waves. (a) Beach slope of 1/9 to 1/12. (b) Beach slope of 1/20. (c) Beach slope of 1/30. (d) Beach slope of 1/50. (e) Beach slope of 1/100 to 1/200. (f) Breaker index on horizontal bed in a narrowing flume by Danel (1951).

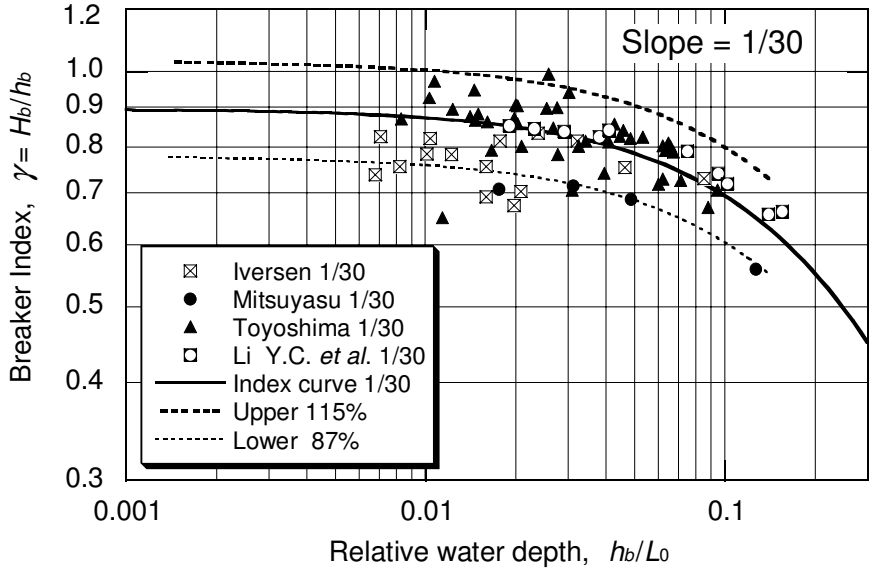

(c)

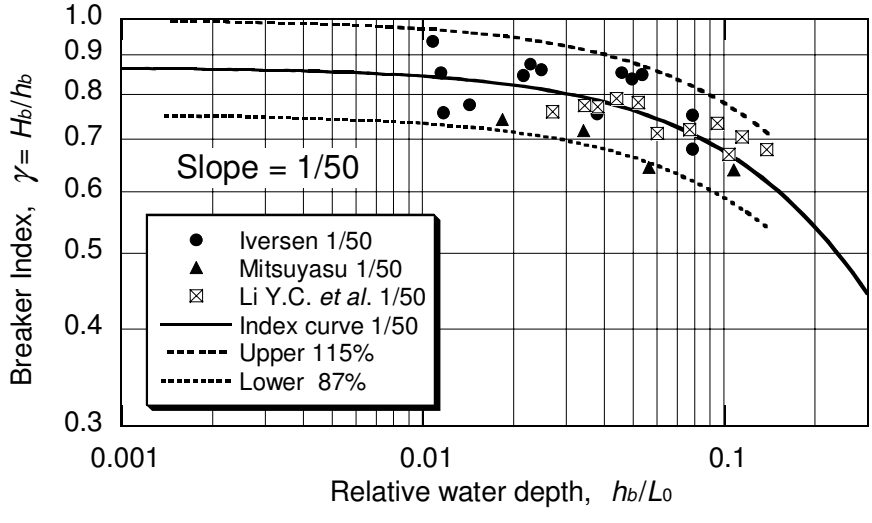

(d)

Fig. 1. (*Continued*)

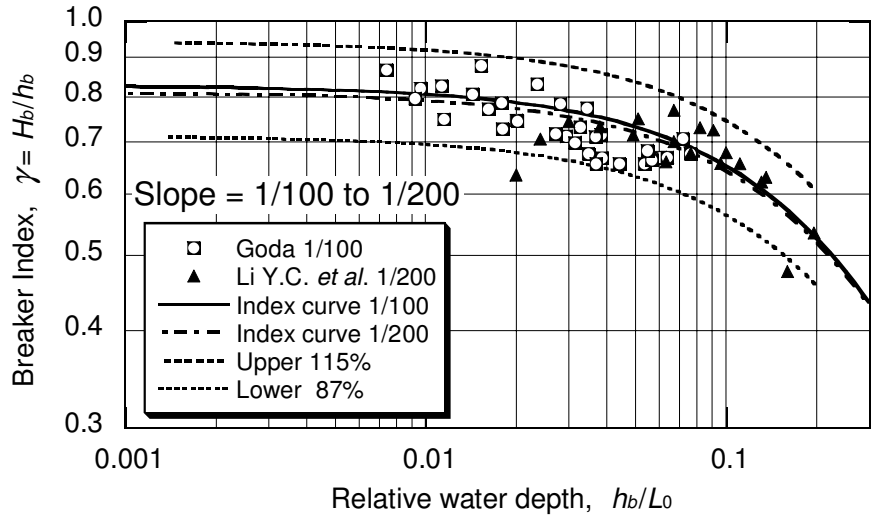

(e)

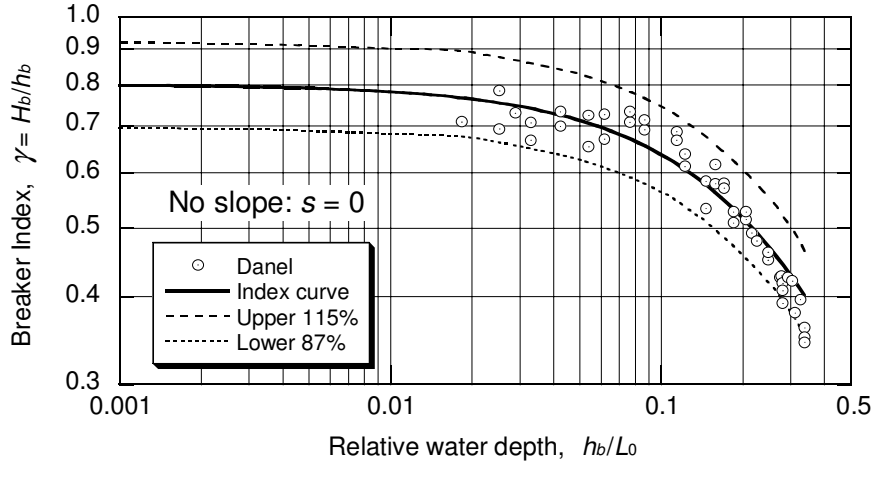

(f)

Fig. 1. (*Continued*)

Figure 1 clearly indicates that the value of the breaker index increases as the beach slope becomes steep. Thus, it is absolutely necessary to incorporate the slope effect into the breaker index formula. Because the experimental data are scattered around the index curves, the upper and lower bound curves corresponding to 115% and 87% of the value by Eq. (6) are drawn in Fig. 1.

2.4. *Variability of breaker index data of regular waves*

A quantitative evaluation of the degree of the scatter is made by means of the relative error of the breaker index, i.e.

$$E = 1 - \frac{\gamma_{\text{mean}}}{\gamma_{\text{est}}} \tag{7}$$

where γ_{meas} is the measured value of H_b/h_b and γ_{est} is the predicted value by the breaker index formula of Eq. (6). The mean and the standard deviation of the relative error are calculated for each group of the beach slope. The mean E_{mean} indicates a bias of the breaker index and the standard deviation of E represents the degree of scatter of the breaker index. A positive bias indicates a tendency of overestimate, while a negative bias shows an underestimate. Because E is defined as the relative error, the standard deviation $\sigma(E)$ is equivalent to the coefficient of variation (CoV). Table 2 lists the bias and CoV of the breaker index of Eq. (6) for the data of various beach slopes. The slope data of 1/9 and 1/12 are excluded from the analysis because of their small sample sizes.

Table 2. Bias and CoV of the breaker index formula of Eq. (6).

Beach slope	Nos. of data	Bias = E_{mean}	$CoV = \sigma(E)$	Sources
1/10	29	−0.5%	14.0%	Iversen, Goda *et al.*
1/20	47	+3.9%	11.3%	Iversen, Galvin, Toyoshima *et al.*, Lara *et al.*
1/30	73	+1.4%	8.6%	Iversen, Mitsuyasu, Toyoshima *et al.*, Li *et al.*
1/50	28	−2.9%	4.8%	Iversen, Mitsuyasu, Li *et al.*
1/100	32	+6.2%	5.5%	Goda
1/200	19	+3.5%	7.4%	Li *et al.*
0	46	+1.7%	6.3%	Danel

The bias varies from −2.9% to +6.2% depending on the beach slope, and the overall mean bias is +1.9%. Because of the small bias, Eq. (6) can be regarded as yielding reasonable estimates of the breaker heights. The scatter of the data as expressed by CoV is about 5% to 7% for the beach slope of zero to 1/50, it increases as the slope becomes steep, and it takes the value of 14% for the beach slope of 1/10. Such scatter of data represents an inherent stochastic nature of wave breaking phenomenon. It resides in the dataset itself, being independent of the breaker index formula being applied.

Even under a well-controlled laboratory test, the breaking point fluctuates over some distance and the breaker height varies from wave to wave. Smith and Kraus [1991] reported on their regular wave tests that "despite care in conducting the tests and use of the average value of the given quantity (i.e. over ten waves), wide scatter appeared in some quantities and must be considered inherent to the breaking process of realistic waves." One cause of the data scatter is the presence of small-amplitude, long-period oscillations of water level in a laboratory flume, but the breaking process itself is triggered by many small factors beyond the control of experimentalists.

With such a degree of inherent variability, it is difficult to select the best fitting breaker index formula among several candidates and the arguments on superiority of one formula to others will not be productive. It should suffice for engineering applications that the selected function has the least bias over a wide range of beach slopes and relative depth. We should regard the wave breaking phenomenon as a stochastic one and accept a certain range of natural fluctuation. As listed in Table 2, the coefficient of variation is large for steep slope and it become small for gentle slope. In any research work involving wave breaking phenomena, due consideration should be given to such stochastic nature of breaker heights. The reliability assessment of maritime structures should also be made by taking into account the statistical variability of breaker heights as a source of uncertainty in design parameters.

2.5. *Variability of breaker index of irregular waves*

The first effort to identify the breaker heights of individual waves among trains of irregular waves was undertaken by Kimura and Seyama [1986] and Seyama and Kimura [1992], who analyzed about 1,000 individual breaking waves for each one of the beach slopes of 1/10, 1/20, 1/30, and 1/50 with the aid of a video camera and wave gauges. The breaker index of individual waves varied over a wide range, which was equivalent to CoV of 18% to 23% (the present author's visual inspection of scatter diagrams). In order to reduce the scatter of data, they proposed to employ an artificial water depth below the mid-level between the wave crest and trough of individual breaking waves and reduced CoV to the values between 8% and 11%. Because Eq. (1) yielded the value of breaker index larger than most of the observed value, they proposed its modified version. When the revised breaker index formula of Eq. (6) is employed, however, the center line of the scatted data appears to be at the level of 85% ($s = 1/10$) to 95% (for other slopes) of the predicted value.

Black and Rosenberg [1992] made observation of individual breaking waves on a natural beach with the depth of 1.0 to 1.5 m at Apollo Bay in southern Australia. The median value of the breaker index was about 84% and 87% of those by Eqs. (1) and (6), respectively.

Another observation was made by Kriebel [2000] in a large wave flume with a bed slope of 1/50 for waves with the significant height of 0.46 m and the peak period of 2.9 s. When he applied Eq. (1) to individual breaker heights, he found that the value of the proportionality coefficient A fitted to the data varied from about 0.09 to 0.18 with a mean of 0.142 (84% of Eq. (1)) and the standard deviation of 0.017 (equivalent to CoV of 12%). Li *et al.* [2000b] also reported the result of their measurements of random breaking waves on the slope of 1/50 and 1/200, recommending the coefficient value of $A = 0.150$ with the standard deviation of 0.031.

It should be recalled that the random wave breaking model by Goda [1975] had already incorporated the variability of breaker heights by assigning a variable probability of individual wave breaking. The probability was assumed to increase

linearly from 0 to 1 in the range of the wave height from 71% to 106% of the height predicted by Eq. (1), corresponding to $A = 0.12$ to 0.18. Therefore, it is expected that the median value of individual breaker heights would be smaller than those predicted by Eq. (1) or (6).

3. Breaker Index for Characteristic Heights of Random Waves

3.1. *Incipient breaking of significant waves by Kamphuis*

Equations (1) and (6) are examples of the breaker index for *regular waves*. There are some people who try to apply such breaker index formulas to coastal waves or *random waves*, but such application does not yield correct answers. The breaker index for regular waves may be utilized for the highest wave in an irregular wave train, but it cannot be applied for the significant wave, the root-mean-square wave, or any other characteristic wave. When random waves approach the shore, breaking of individual waves occurs gradually with large waves first at the far distance, medium waves next at some distance from the shore, and small waves near the shoreline. The variation of significant wave height from the offshore toward the shore is so gradual that we cannot employ the concept of wave breaking line, which is quite obvious in the case of regular waves.

Against such difficulty of defining the breaking point of significant wave, Kamphuis [1991] introduced a definition of "incipient wave breaking." He measured cross-shore variations of significant wave height beyond and across the surf zone, drew a curve of wave shoaling trend in the outside of the surf zone and a curve of wave height decay within the surf zone. Then he called the condition at the cross point of the two curves as the incipient wave breaking. By using the data of the significant wave height at incipient breaking, he calibrated eleven breaker index formulas and determined the best-fitting proportionality coefficient. For the formula of Eq. (1), he obtained the proportionality coefficient of $A = 0.12$ for significant wave height.

Li *et al.* [2000b] have also presented a data of the breaker index of $(H_{1/3}/h)_b$ on the slope of 1/200, which is fitted to Eq. (1) with a modified constant value of 0.12 for the initial stage of breaking. Their breaking condition was some observation of breaking of a few large individual waves in an irregular wave train.

Goda [1975] has prepared a set of diagrams depicting variations of significant wave height across the surf zone (reproduced as Figs. 3.29 to 3.32 in Goda [2000]). These diagrams are marked with the boundary lines of 2% decay of wave heights, beyond which the attenuation of wave heights by random wave breaking causes more than 2% decay in comparison with the nonlinear shoaling heights. The water depth at these boundary lines approximately correspond to the breaker index with $A = 0.10$ to 0.12. Goda [1975] also prepared two diagrams for the peak value of significant wave height $(H_{1/3})_{\text{peak}}$ within the surf zone and the water depth $(h_{1/3})_{\text{peak}}$ at which $(H_{1/3})_{\text{peak}}$ occurs (Figs. 3.34 and 3.35 of Goda [2000]). The locations of the peak significant wave height approximately correspond to $A = 0.11$ to 0.13. These

locations can be regarded to correspond to the incipient breaking of significant wave breaking. Therefore, the incipient breaker index of the significant wave can be expressed with the following formula:

$$\left(\frac{H_{1/3,b}}{h_b}\right)_{\text{incipient}} = \frac{0.12}{h_b/L_0}\left\{1-\exp\left[-1.5\pi\frac{(h_b)_{\text{incipient}}}{L_0}(1+11s^{4/3})\right]\right\} \tag{8}$$

The incipient breaker index of significant wave is about 30% lower than that of regular waves in terms of the A value. Because the water depth $(h_{1/3})_{\text{peak}}$ is shallower than the depth of 2% decay line, it is estimated that the percentage of breaking waves at the incipient breaking would be several percent.

3.2. *Breaker index of significant waves within the surf zone*

As waves progress toward the shoreline, the percentage of breaking waves increases and the ratio of the significant wave height to the water depth, $H_{1/3}/h$, gradually increases from the incipient breaker index. Figure 2 exhibits examples of $H_{1/3}/h$ taken from the laboratory data of Tominaga and Hashimoto [1972] for $s = 1/70$, Goda [1975] for $s = 1/50$, and Ting [2001, 2002] for $s = 1/35$. Table 3 lists a summary of the test conditions of these data.

The breaker index curves with $A = 0.12$, 0.15, and 0.18 for $s = 1/50$ are also plotted in Fig. 2. The laboratory data with the relative depth of $h/L_0 = 0.05$ to 0.10 are located in the zone of $A = 0.11$ to 0.14, while the data with $h/L_0 = 0.01$

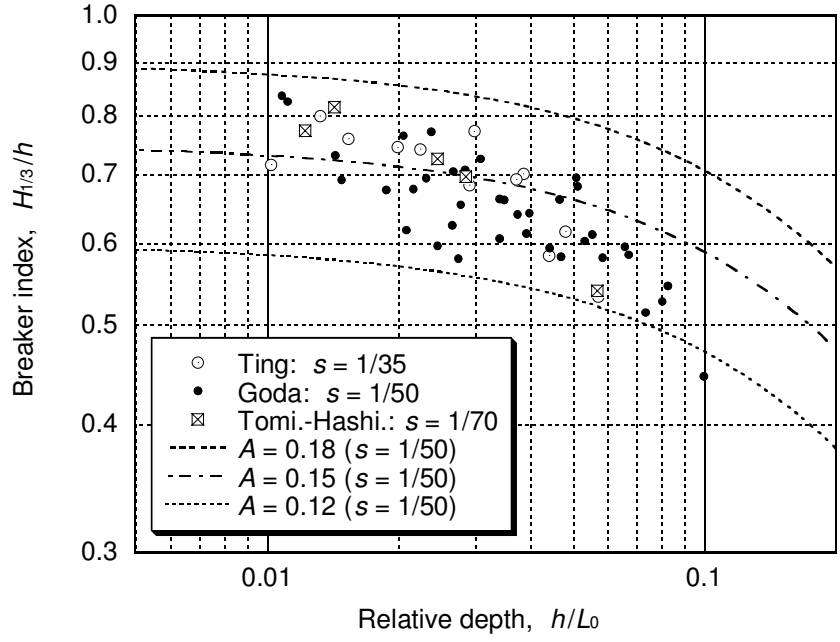

Fig. 2. Laboratory data of breaker index of significant wave height in the surf zone.

Table 3. Summary of laboratory data sets of random wave breaking.

Authors	Beach slope	Nos. data	$T_{1/3}$ (s)	H_0' (cm)	Depth h (cm)	Statistical height (cm)	Value of A
Tominaga and Hashimoto [1972]	1/70	5	1.5	11.5	20.0–4.3	$H_{1/3} = 10.8$–3.32	0.13–0.17
Goda [1975]	1/50	37	1.0–1.9	8.5–12.1	25.0–6.0	$H_{1/3} = 10.3$–3.86	0.11–0.17
Ting [2001, 2002]	1/35	12	1.7, 2.0	14.2	27.0–6.3	$H_{1/3} = 15.8$–4.47	0.12–0.16
Battjes [1972]	1/20	14	1.3, 2.2	$\simeq 12$	15.9–4.1	$H_{\rm rms} = 9.3$–3.54	0.08–0.20
Ting [2001, 2002]	1/35	12	1.7, 2.0	14.2	27.0–6.3	$H_{\rm rms} = 11.4$–3.58	0.09–0.12

Table 4. Summary of stationary coastal wave data employed in the present analysis (Source: Goda and Nagai [1974]; Goda [1975]; and Goda [1983a]).

Observation station	Type of wave gauge	Water depth (m)	Sampling interval Δt (s)	Significant height $H_{1/3}$ (m)	Significant period $T_{1/3}$ (s)	Nos. of data
Rumoi Port	Step-resistance	−11.5	0.5	2.2–7.1	5.9–11.7	44
Yamase-Domari Port	ditto	−12.7	0.5	1.9–6.2	7.7–15.6	9
Tomakomai Port	ditto	−10.8	1.0	2.9–5.8	7.7–10.9	9
		−13.8	0.5	2.6–2.8	6.7–7.5	2
ditto	Ultrasonic	−20	0.5	2.4–2.5	6.9–7.4	2
Kanazawa Port	ditto	−20	1.0	1.0–6.8	1.0–6.8	13
Caldera Port, Costa Rica	ditto	−18	0.5	1.5–3.6	14.2–18.4	50
Sakata Port	Pressure	−14.5	0.5	1.7–9.7	6.3–13.4	123
		−10.5		1.7–6.1	6.5–15.0	123

to 0.02 correspond to the zone of $A = 0.14$ to 0.17. The leftward shift of data position in the abscissa of h/L_0 in Fig. 2 has occurred mainly by the decrease of the water depth: i.e. shift of measuring point toward the shoreline. Thus, Fig. 2 clearly indicates gradual increase of the breaker index of $H_{1/3}/h$ from the incipient index value within the surf zone.

Similar tendency of the increase of the breaker index of $H_{1/3}/h$ has been observed in the field data as shown in Fig. 3. The data are composed of two groups: coastal wave station data and photopole data; the name of "photopole" was adopted by Ebersole and Hughes [1987]. The former is the data selected from the records of stationary wave measurements as listed in Table 4, and the latter is the photogrametric measurement data by Hotta and Mizuguchi [1980, 1986] and Ebersole and Hughes [1987] as listed in Table 5. Coastal wave data were measured with step-resistance gauges, ultrasonic wave sensors (inverted echo-sounder), or pressure gauges (Sakata

Table 5. Summary of photopole measurements.

Name	Date	Nos. of data	h (m)	H_0 (m)	$T_{1/3}$ (s)	H_0/L_0
Ajigaura	1978/09/05	54	0.6–2.7	0.7	8.4	0.0064
	1978/12/13-14	175	0.1–1.8	0.5–0.7	7.2–7.9	0.0059–0.0081
DUCK85	1985/09/04-05	99	0.5–2.4	0.3–0.5	10.3–11.1	0.0017–0.0028
SUPERDUCK	1986/09/11-19	140	0.4–3.7	0.5–1.1	5.4–11.5	0.0027–0.0254

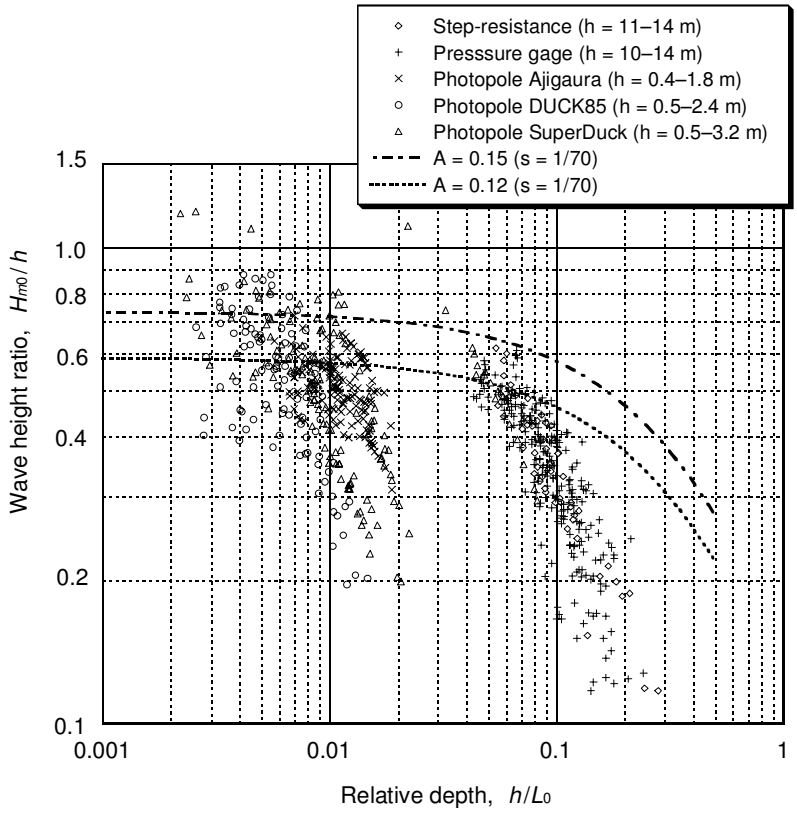

Fig. 3. Field data of H_{m0}/h outside and inside the surf zone.

Port), and they represent several sequences of two-hourly records of storm waves. Although there remains a problem of pressure conversion to surface profiles in the case of the Sakata data, the conversion error would have been small because of the relatively shallow water depth of 10.5 and 14.5 m. The wave data by ultrasonic wave sensors are not employed in Fig. 3, but will be utilized in the wave nonlinearity analysis in Sec. 5.

The photopole data were obtained through the frame-by-frame analysis of water surface elevations at multiple poles elected perpendicularly to the shoreline from

the films of multiple motion-picture cameras. Hotta and Mizuguchi [1980, 1986] measured waves at Ajigaura Beach, Ibaragi, Japan by erecting about sixty poles over 120 m and mobilizing eleven cameras on top of a coastal observation pier. Ebersole and Hughes [1987] used the photopole technique on occasion of DUCK85 campaign in Duck, North Carolina, USA with cooperation of Dr. Hotta who brought six cameras with him and took charge of filming. They erected twelve poles over 64 m and used six motion-picture cameras. Another series of the photopole measurements was made during SuperDuck campaign by erecting twenty poles, the data of which were kindly provided to the present author by Dr. Hughes.

The data plotted in Fig. 3 include both non-breaking waves outside the surf zone and breaking waves inside the surf zone, because identification of wave breaking phenomenon is not possible for the statistically analyzed data. The objective of plotting all the data is to explore the possibility of finding out a kind of an upper envelope curve that may represent the breaker index value. The spectral significant wave height of Eq. (9) is employed in Fig. 3 instead of the zero-crossing significant wave height $H_{1/3}$.

$$H_{m0} = 4.004\eta_{\rm rms} = 4.004\sqrt{m_0} \tag{9}$$

where m_0 denotes the zero-th spectral moment.

Difference between H_{m0} and $H_{1/3}$ has been discussed over years. The present paper deals with the problem from the viewpoints of the spectral shape effect in Sec. 4.2 and the wave nonlinearity effect in Sec. 5.2. Use of H_{m0} in Fig. 3 is so made to minimize the influence of spectral shape and wave nonlinearity effect on data plotting.

Figure 3 indicates four outliers above the line of $H_{m0}/h = 1.0$; they belong to the shallowest pole during SuperDuck campaign. The water depth h of the photopole data were estimated with the mean water level calculated from the instantaneous surface elevations. The cause of the four outliers is not known. Excluding these outliners, however, Fig. 3 indicates that most of the H_{m0}/h data are located below the breaker index curve with $A = 0.18$ and they tend to spread above the index curve with $A = 0.15$ as the relative depth decreases. It is the same tendency as the laboratory data. Thus, it is concluded that the breaker index for the significant wave height increases gradually inside the surf zone from the incipient value of Eq. (7).

It is seen that the spectral significant wave height H_{m0} on gentle slopes does not exceed 0.7 times the local water depth except for the low-steepness swell in very shallow water. For the range of $h/L_0 > 0.03$, the upper limit of significant wave height is about 0.6 times the local water depth.

3.3. *Breaker index of* $H_{\rm rms}$

As for the breaker index of $H_{\rm rms}$, Fig. 4 shows the variation of $H_{\rm rms}/h$ with the relative depth h/L_0 for the laboratory data by Battjes [1972] for $s = 1/20$ and Ting

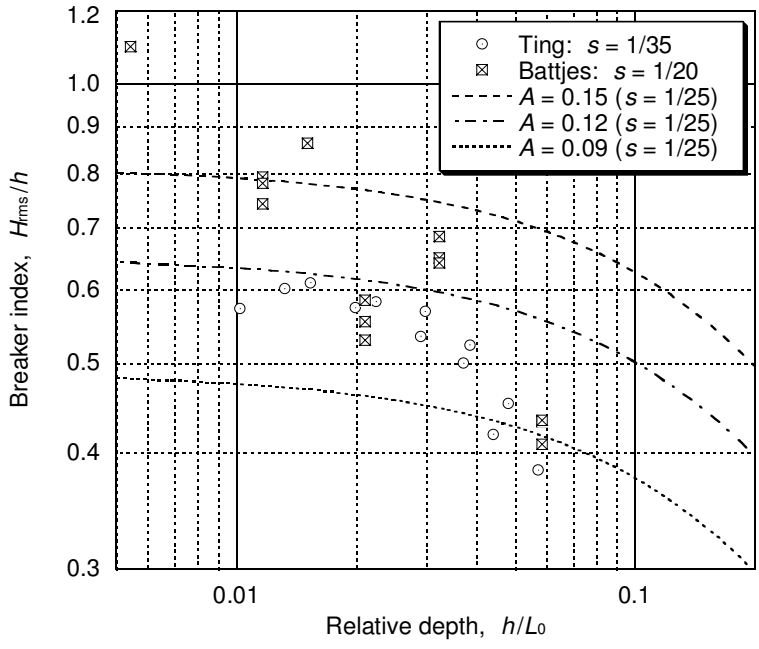

Fig. 4. Laboratory data of breaker index of root-mean-square wave height in the surf zone.

[2001, 2002] for $s = 1/35$; the summary of these data has been listed in Table 3. When the relationship of $H_{\rm rms} = 0.706 H_{1/3}$ under the Rayleigh distribution is applied, the coefficient value of $A = 0.12$ for $H_{1/3}$ in Eq. (7) is converted to $A = 0.084$ for $H_{\rm rms}$. In comparison with three index curves of $A = 0.09$, 0.12, and 0.15 in Fig. 4, the laboratory data support the incipient index value of $A = 0.084$ for $H_{\rm rms}$, but the data indicate an increase of the A value as the relative depth decreases. It is the same tendency as the case of significant wave height.

The breaker index data for $H_{\rm rms}$ in Fig. 4 is higher than the value proposed by Sallenger and Holman [1985], who gave an expression of $H_{\rm rms}/h = 3.2\ s + 0.32$ without inclusion of the relative depth (h/L_0) term. They converted the orbital velocity spectra to the surface wave spectra with the transfer function based on the linear theory, and estimated the spectrum-based $H_{\rm rms}$, which must have been smaller than the statistical $H_{\rm rms}$ value based on direct measurement data of surface profiles. Thus, the formula by Sallenger and Holman [1985] is not recommended for application to the random wave breaking model.

4. Evolution of Wave Height Distribution Function across the Surf Zone

4.1. *Rayleigh distribution of individual wave heights*

Longuet-Higgins [1952] has demonstrated the applicability of Rayleigh distribution to the heights of sea waves when the frequency spectrum is narrow banded. Since

then, many field observations have shown that wave heights defined by the zero-crossing method approximately follow the Rayleigh. When the Rayleigh distribution holds, various characteristic wave heights are theoretically calculated in terms of the spectral significant wave height H_{m0}. The following are some examples:

$$H_{1/10} = 1.27H_{m0}, \quad H_{1/3} = H_{m0}\,, \quad H_{\rm rms} = 0.707H_{m0} \tag{10}$$

Applicability of the Rayleigh distribution to zero-crossing wave heights is an approximate one, however. The bandwidth of the frequency spectrum of actual sea waves is not narrow but broad, and the functional shape of frequency spectrum brings forth a certain deviation of wave heights from the Rayleigh as discussed in the next subsection. As waves propagate in shoaling waters toward the shore, individual wave heights are enhanced by the nonlinear shoaling process and the wave height distribution becomes broader than the Rayleigh. This aspect is discussed in Sec. 5.2. After waves enter the surf zone, the random wave breaking process strongly modifies the wave height distribution as discussed in Secs. 4.3 and 4.4.

4.2. *Effect of spectral shape on wave height distribution*

The effect of the frequency spectral shape on the wave height distribution has been discussed by many researchers. Among them, Goda and Kudaka [2007] have employed the following spectral shape parameter for examining wave height distribution:

$$\kappa(\bar{T})^2 = \left|\frac{1}{m_0}\int_0^\infty S(f)\cos 2\pi f\bar{T}df\right|^2 + \left|\frac{1}{m_0}\int_0^\infty S(f)\sin 2\pi f\bar{T}df\right|^2 \tag{11}$$

where $\bar{T}$ denotes the mean wave period and $S(f)$ is the frequency spectral density. The mean wave period may be defined as $\bar{T} = T_{0,1} = m_0/m_1$ where m_1 denotes the first spectral moment. The value of the spectral shape parameter $\kappa(\bar{T})$ approaches 1.0 as the spectral peak becomes sharp, and it goes down to 0 for a flat spectrum. On the basis of simulated wave profile data and field measurement data, Goda and Kudaka have given an empirical formula for the ratio $H_{1/3}/H_{m0}$ as follows:

$$H_{1/3}/H_{m0} = 0.864 + 0.338\kappa - 0.346\kappa^2 + 0.144\kappa^3 \tag{12}$$

For most of the wind waves and swell in relatively deep water, the spectral shape parameter takes the value between 0.3 and 0.5, which yields the $H_{1/3}/H_{m0}$ value of 0.94 to 0.96. The majority of wave observation data indicates that the zero-crossing significant wave height $H_{1/3}$ is 5% smaller than the spectral significant height H_{m0} on average, or $H_{1/3} \approx 0.95H_{m0}$ (see Goda [1979] for example). This relationship will be used as a benchmark when discussing wave nonlinearity effect.

4.3. *Probability density function of wave heights in the surf zone*

The probability density function (*pdf*) of wave heights provides the basis for calculating various characteristic wave heights such as $H_{\rm max}$, $H_{2\%}$, $H_{1/10}$, $H_{1/3}$, $H_{\rm rms}$ and

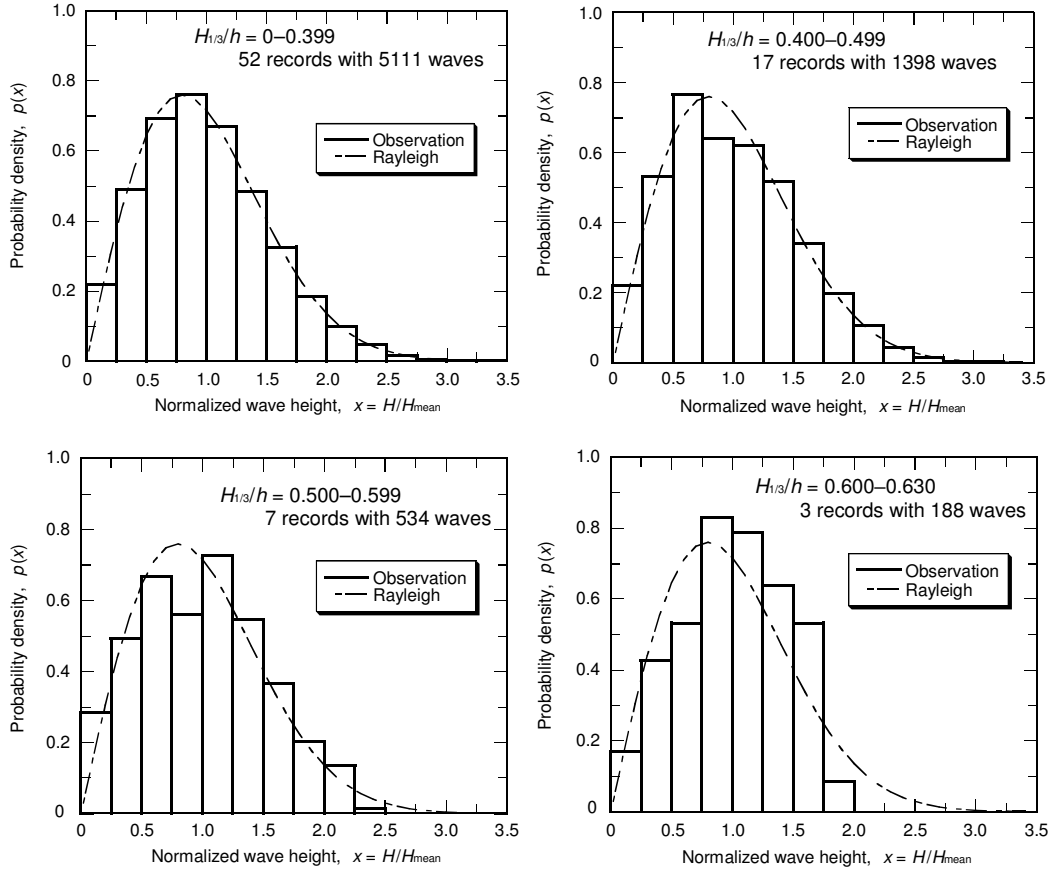

Fig. 5. Histograms of field wave data in four groups of relative water depth after Goda [1975].

others. Information on these characteristic wave heights is indispensable in design of breakwaters and other structures. For example, composite breakwaters are designed against $H_{\max}$ while armor stone size is selected against $H_{2\%}$. Beach morphological problems are often analyzed with the input of $H_{\rm rms}$ and/or $H_{1/3}$, but their mutual relationship in shoaling waters may deviate from the prediction under the Rayleigh distribution of wave heights.

Figure 5 shows examples of the evolution of the probability density function (*pdf*) of wave heights on the basis of some of the coastal station data listed in Table 4; Fig. 5 has been taken from Goda [1975]. The data are presented in four groups according to the value of the ratio of the zero-crossing significant wave height to the water depth, $H_{1/3}/h$. For each group, individual wave heights are normalized with the mean wave heights of respective wave records and the histogram of wave heights is constructed in the form of probability density function (*pdf*). The group with $H_{1/3}/h < 0.4$ demonstrates the wave heights being in good agreement with the Rayleigh distribution. Though not discernible in the figure, there is a small number

of waves in the class of $H/H_{\mathrm{mean}} = 3.25$ to 3.50, corresponding to the probability density of the Rayleigh. The next group with $0.4 \leq H_{1/3}/h < 0.5$ does not have any wave in the class of $H/H_{\mathrm{mean}} > 3.25$ and the histogram indicates a slight leftward shift. As the relative wave height increases, disappearance of large individual waves becomes clearer and so is the deviation from the Rayleigh distribution. The two groups with $H_{1/3}/h > 0.5$ are regarded as waves within the surf zone with reference to Figs. 2 and 3.

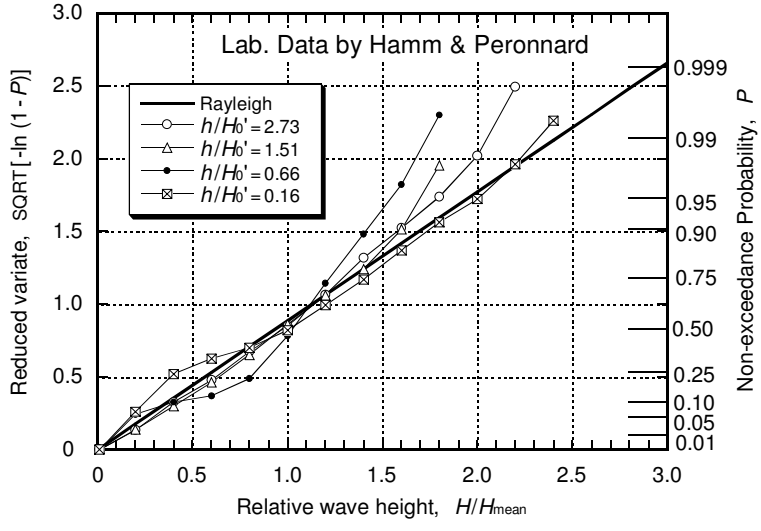

(a)

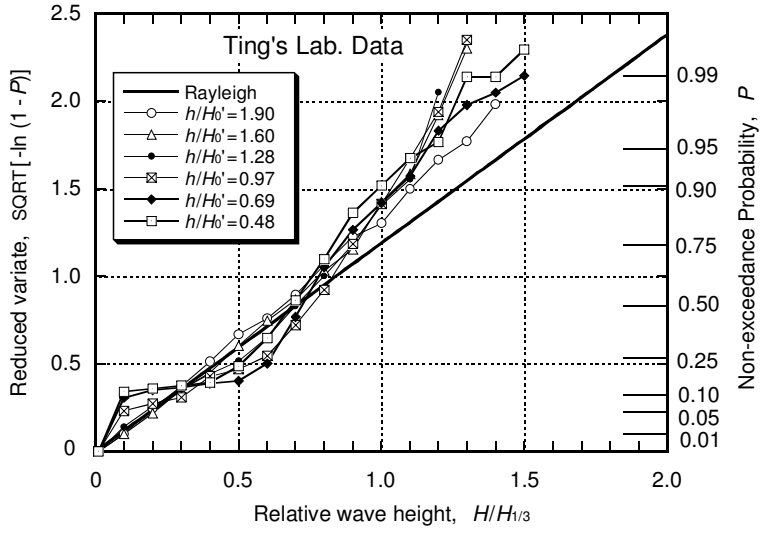

(b)

Fig. 6. Evolution of cumulative distribution of wave heights in the surf zone. (a) Laboratory data by Hamm and Peronnard [1997]. (b) Laboratory data of Ting [2001].

Through laboratory tests, Hamm and Peronnard [1997] and Ting [2001] also presented examples of wave height histograms across the surf zone. Their data are re-plotted in the form of cumulative distribution as shown in Fig. 6. The abscissa is the relative wave height H/H_{mean} or $H/H_{1/3}$, while the ordinate is the reduced variate of $[1-\ln(1-P)]^{1/2}$, where P denotes the non-exceedance probability of wave heights. If the wave heights follow the Rayleigh distribution, they will be plotted along the straight line shown in Fig. 6.

Both the data in Fig. 6 show a departure of cumulative distribution from the Rayleigh as the ratio of the water depth to the deepwater wave height, h/H_0', decreases. Departure is exhibited by the shift of the upper part of the cumulative distribution toward the left, i.e. lowering of large waves. The largest departure is observed around $h/H_0' = 1.0$. As the ratio h/H_0' further decreases, the cumulative distribution shows a tendency to return to the Rayleigh again. The tendency is most conspicuous for the data of $h/H_0' = 0.16$ by Hamm and Pernonnard.

4.4. *Evolution of wave height ratios* $H_{2\%}/H_{1/3}$, $H_{1/10}/H_{1/3}$ *and* $H_{\mathrm{rms}}/H_{1/3}$

Gradual change of the *pdf* of wave heights also modifies the ratios between the characteristic wave heights defined by the zero-crossing method. Figure 7 shows the laboratory data on the variation of the wave height ratios $H_{2\%}/H_{1/3}$ and $H_{\mathrm{rms}}/H_{1/3}$ with respect to the relative depth h/H_0'. The zero-crossing significant wave height

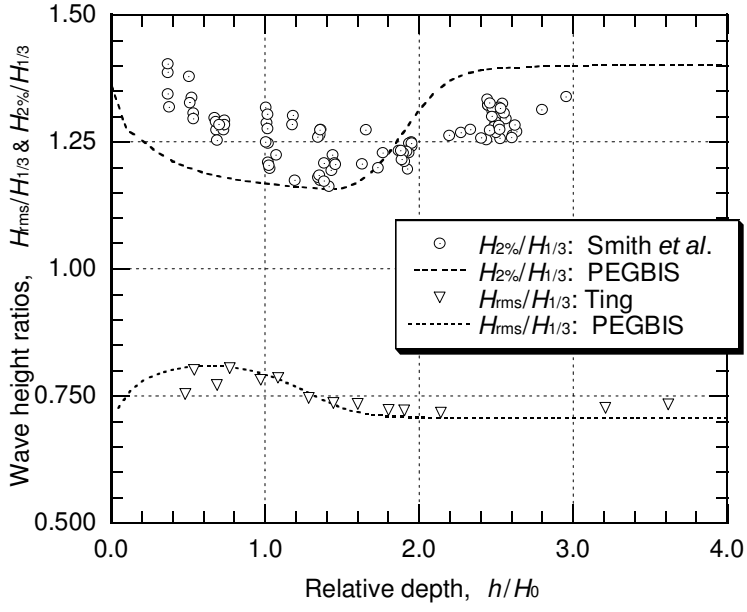

Fig. 7. Laboratory data of variations of wave height ratios $H_{2\%}/H_{1/3}$ and $H_{\mathrm{rms}}/H_{1/3}$ across the surf zone.

$H_{1/3}$ is employed as the denominator to minimize the wave nonlinearity effect on wave height ratios.

The data of $H_{2\%}/H_{1/3}$ are from Smith *et al.* [2002] on $s = 1/100$, and the data of $H_{\rm rms}/H_{1/3}$ are from Ting [2001, 2002] on $s = 1/35$. The data by Smith *et al.* are composed of single- and double peaked spectral waves, but they are shown here without differentiation because of little appreciable difference. Predictions of the variation of these wave height ratios by the wave transformation model PEGBIS by Goda [2004] are also shown in Fig. 7.

Figure 7 clearly demonstrates a narrowing of the wave height distribution in the middle of the surf zone with decrease of the $H_{2\%}/H_{1/3}$ value and increase of the $H_{\rm rms}/H_{1/3}$ value, and a widening of the distribution in the area near the shoreline. The decrease of $H_{2\%}/H_{1/3}$ is largest around $h/H_0 \approx 1.4$, while the increase of $H_{\rm rms}/H_{1/3}$ is largest around $h/H_0 \approx 0.8$; difference is partly due to the beach slopes employed in the tests. Prediction by the PEGBIS model exhibits some difference from the laboratory data for the case of $H_{2\%}/H_{1/3}$, but the model demonstrates the capacity to reproduce the variations of characteristic wave heights across the surf zone.

The photopole data in Table 5 are also analyzed for the variations of $H_{1/10}/H_{1/3}$ and $H_{\rm rms}/H_{1/3}$ across the surf zone as shown in Fig. 8 together with the prediction by the PEGBIS model, which was calculated with the beach slope of $s = 1/70$ corresponding to the condition of Ajigaura Beach. Large scatters of data originate from small sample sizes of wave records (650 to 760 s long and 60 to 100 waves per

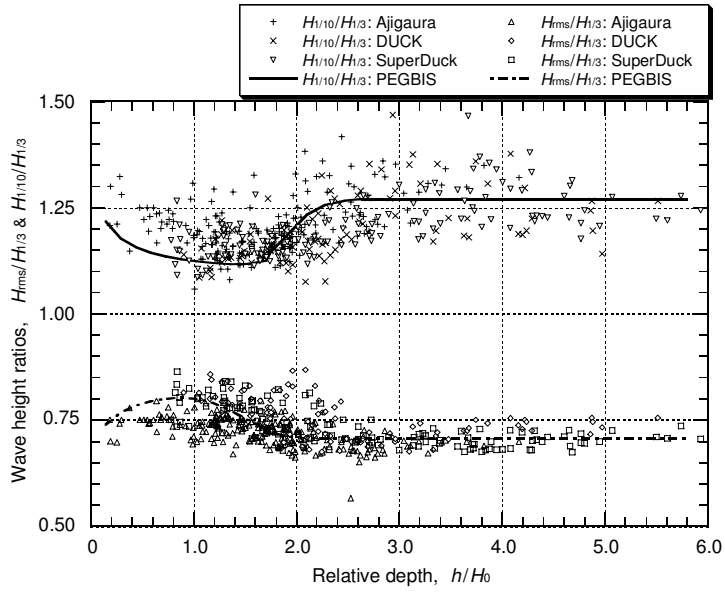

Fig. 8. Field data of the variations of wave height ratios $H_{10}/H_{1/3}$ and $H_{\rm rms}/H_{1/3}$ across the surf zone.

record); the 90% confidence interval of the wave height ratios is estimated as ±10% (e.g. Goda [1988]).

The ratio $H_{1/10}/H_{1/3}$ takes the minimum value of about 1.15 around $h/H_0 = 1.4$, which indicate slightly larger values than the PEGBIS prediction probably owing to the wave nonlinearity effect. The ratio $H_{\rm rms}/H_{1/3}$ takes the maximum value of about 0.81 around $h/H_0 = 1.0$. The DUCK85 data exhibit the $H_{\rm rms}/H_{1/3}$ being closer to 1 than the Ajigaura data. It might be due to lower wave steepness of the swell at DUCK85.

Variation of the wave height ratios across the surf zone are the result of gradual change of the *pdf*. Return of the *pdf* to the Rayleigh near the shoreline owes to wave regeneration after the breaking of large waves. Increase of the surf beat amplitude near the shoreline is considered to contribute to the widening of the *pdf* as discussed by Goda [1975].

Battjes and Groenenkijk [2000] have proposed a composite Weibull distribution for the wave heights in the surf zone, which is a combination of the Rayleigh distribution for lower waves and a Weibull distribution with the shape parameter of $k = 3.6$ and a null location parameter for higher waves. They claim to be able to fit the composite distribution to a measured one by adjusting the transition height of the two distributions. However, their model distribution cannot deal with the actual process of wave height distribution transformation such that the distribution returns to the Rayleigh near the shoreline.

Any numerical wave transformation model with random breaking is asked to have the capability of appropriately reproducing the gradual change of the *pdf* and the associated variation of wave height ratios across the surf zone such as those discussed in the above. A phase-averaging type model with a single wave height parameter such as $H_{\rm rms}$ cannot predict a deformation of the *pdf*, and the model may not function well in engineering applications for structure designs.

5. Wave Nonlinearity across the Surf Zone

5.1. *Skewness and kurtosis of surface elevation*

Ocean waves are characterized with almost linear behaviors, as evidenced by the Gaussian distribution of surface elevation. Wave linearity is the basis of spectral representation and analysis. Deviation from the linearity is measured with the values of the skewness and the kurtosis of the surface elevation with reference to the mean water level during a wave record; they are defined as below.

$$\text{Skewness}: \quad \beta_1 = \frac{1}{\eta_{\rm rms}^3} \cdot \frac{1}{N} \sum_{i=1}^{N} (\eta_i - \bar{\eta})^3 \tag{13}$$

$$\text{Kurtosis}: \quad \beta_2 = \frac{1}{\eta_{\rm rms}^4} \cdot \frac{1}{N} \sum_{i=1}^{N} (\eta_i - \bar{\eta})^4 \tag{14}$$

The skewness is zero when a distribution is symmetric with respect to the mean, and takes a positive value when a distribution is asymmetric with a long tail toward the right side (large value). The kurtosis takes a value of 3.0 for the Gaussian distribution. When the mode of distribution has a sharp peak and the distribution has long tails in both the left and right sides, the value of kurtosis becomes much larger than 3.0. The degree of positive skewness and the deviation of kurtosis from 3.0 are the measure of the strength of wave nonlinearity. The skewness of ocean waves is smaller than 0.5 and the kurtosis is below 4.0 for most cases, and thus the nonlinearity of waves in deep water is weak.

The variations of the skewness and kurtosis of field waves are examined with coastal surface waves listed in Table 4 (excluding the pressure sensor data of Sakata Port), and the photopole data in Ajigaura, DUCK85 and SuperDuck listed in Table 5. The data of skewness and kurtosis of September 5th in Ajigaura were kindly provided by Dr. Hotta. The skewness data of the photopole measurements of SuperDuck were presented by Dr. Hughes to the present author.

As waves approach the shore, wave nonlinearity is enhanced and both the skewness and kurtosis increase significantly. Figure 9 exhibits the increase of the skewness with the nonlinearity parameter $\Pi_{1/3}$, which was introduced by Goda [1983b] with the following definition:

$$\Pi_{1/3} = \frac{H_{1/3}}{L_A} \coth^3 \frac{2\pi h}{L_A} \tag{15}$$

where L_A denotes the wavelength corresponding to the significant wave period $T_{1/3}$ to be calculated by the small amplitude wave theory or Airy's theory.

The data are grouped by the range of the offshore wave steepness H_0/L_0: the first group for $0.001 < H_0/L_0 < 0.0029$, the second group for $0.003 < H_0/L_0 < 0.0049$, the third group for $0.0050 < H_0/L_0 < 0.0099$, the fourth group for $0.010 < H_0/L_0 < 0.029$, and the fifth group for $0.030 < H_0/L_0 < 0.049$ (legends are shown with abbreviated figures).

The data shown in the upper diagram of Fig. 9 are those outside the surf zone. Because the boundary of surf zone is difficult to set for random waves, an arbitrary boundary of $h/H_0 = 2.5$ is employed here to separate the wave data outside and inside the surf zone. As shown in the upper diagram, the skewness outside the surf zone shows a clear correlation with the wave nonlinearity parameter. The skewness begins from the value of zero at $\Pi_{1/3} = 0.01$, increases gradually with $\Pi_{1/3}$, and attains the value of 2.0 around $\Pi_{1/3} = 4$. The dashed line represents a semi-theoretical relationship, which is based on the analysis of finite amplitude regular wave profiles by Goda [1983b] with consideration of the occurrence probability of individual wave heights according to the Rayleigh distribution.

Variation of the skewness inside the surf zone ($h/H_0 < 2.5$) is shown in the lower diagram of Fig. 9. The ordinate is the ratio of offshore wave height to water depth, H_0/h, which increases rapidly as waves approach the shore. There is a clear

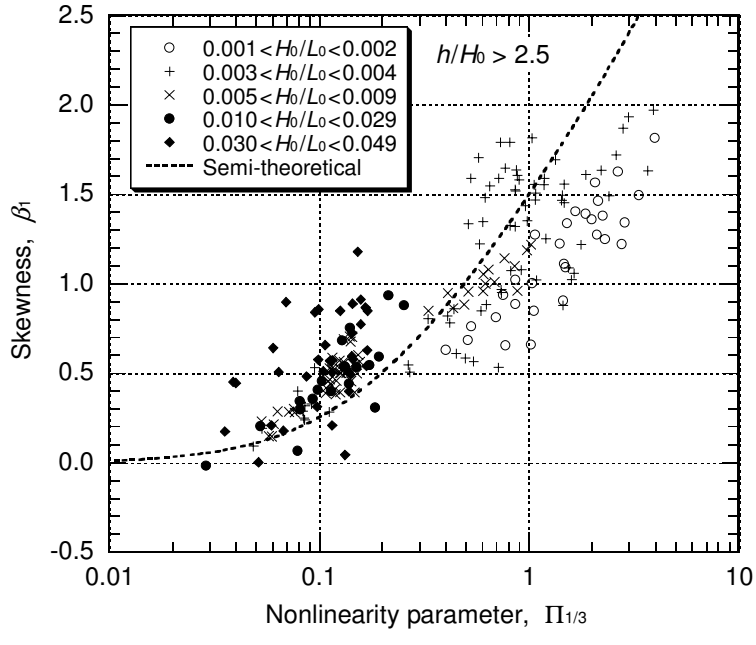

(a)

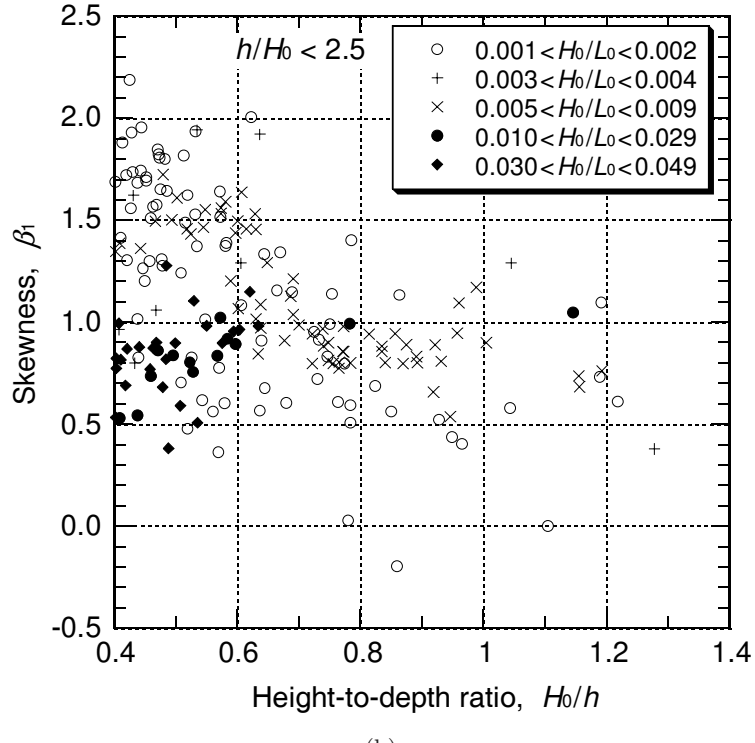

(b)

Fig. 9. Variation of the skewness of surface elevation outside and inside the surf zone. (a) Outside the surf zone ($h/H_0 > 2.5$). (b) Inside the surf zone ($h/H_0 < 2.5$).

trend of decrease of the skewness toward $\beta_1 = 0$ with increase of the height-to-depth ratio H_0/h. Use of the height-to-depth ratio in the lower diagram is to provide a kind of contrast of the increase and decrease of skewness in the outside and inside of the surf zone, respectively. While increase of the skewness outside the surf zone seems indifferent to the wave steepness, the value of skewness inside the surf zone is much affected by the wave steepness; waves of low steepness maintain large values of skewness, while wave of high steepness have small values only.

Variation of the kurtosis of surface elevation is shown in Fig. 10; the upper diagram is for kurtosis outside the surf zone and the lower diagram is for kurtosis inside the surf zone. The pattern of variation is the same as that of skewness, though the available number of kurtosis data is less than the skewness data. The kurtosis starts from the value of 3.0 at $\Pi_{1/3} = 0$, increases as the nonlinearity parameter increases, and attains the value of 9 around $\Pi_{1/3} = 4$. In the lower diagram of Fig. 10, the kurtosis inside the surf zone decreases toward $\beta_2 = 3.0$ as wave approach the shoreline (i.e. increase of H_0/h). Waves with the steepness larger than 0.01 exhibit the kurtosis value much smaller than swell with very low steepness. It is because waves with large steepness cannot experience the full process of nonlinear shoaling owing to the early start of wave breaking.

5.2. *Nonlinear behavior of zero-crossing wave heights against spectral significant height*

Wave nonlinearity is also reflected in individual wave heights defined by the zero-crossing method. In the offshore, individual wave heights almost follow the Rayleigh distribution as discussed in Sec. 4.2. As waves propagate toward the shore, however, waves undergo nonlinear shoaling and wave profiles become skewed with high and sharp crests and low and flat troughs. Because of a skewed wave profile, the potential energy contained in such a profile is smaller than the energy of sinusoidal wave with the same height. In other words, nonlinear waves can have the height much larger than the linear (sinusoidal) waves for the same potential energy.

Owing to the nonlinear shoaling, individual wave heights increase rapidly with the rate greater than that of linear shoaling. Significant wave height and other characteristic wave heights also grow rapidly. The nonlinearity effect becomes most conspicuous around the outer edge of the surf zone. After waves enter the surf zone and begin to be attenuated through breaking process, the wave nonlinearity is gradually lessened. The degree of nonlinear shoaling effect may be judged by a departure of the statistical wave height from the theoretical predictions of Eq. (9) under the Rayleigh distribution.

Figures 11 to 13 show the evolutions of the wave height ratios $H_{1/10}/H_{m0}$, $H_{1/3}/H_{m0}$, and $H_{\rm rms}/H_{m0}$, respectively. The difference between $H_{1/3}$ and H_{m0} in the nearshore waters has been pointed out by several researchers such as Thompson and Vincent [1985] and Ebersole and Hughes [1987]. In these figures, the upper

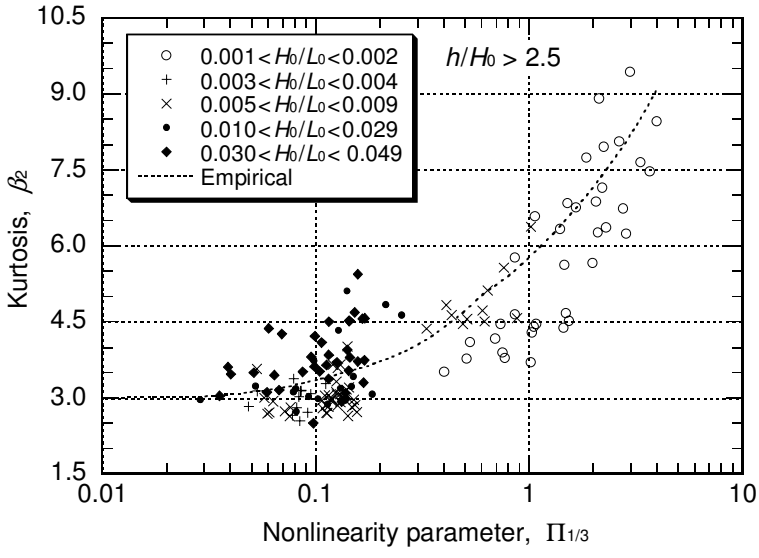

(a)

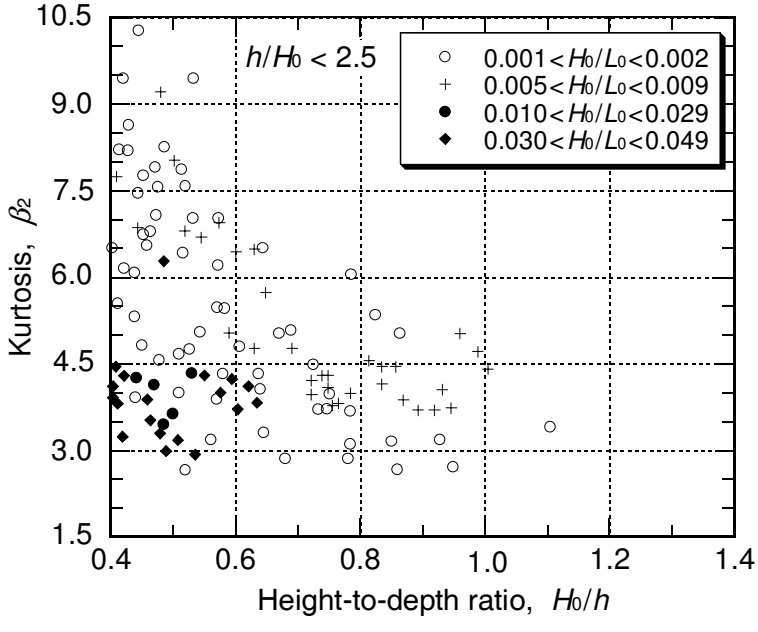

(b)

Fig. 10. Variation of kurtosis of surface elevation outside and inside the surf zone. (a) Outside the surf zone ($h/H_0 > 2.5$). (b) Inside the surf zone ($h/H_0 < 2.5$).

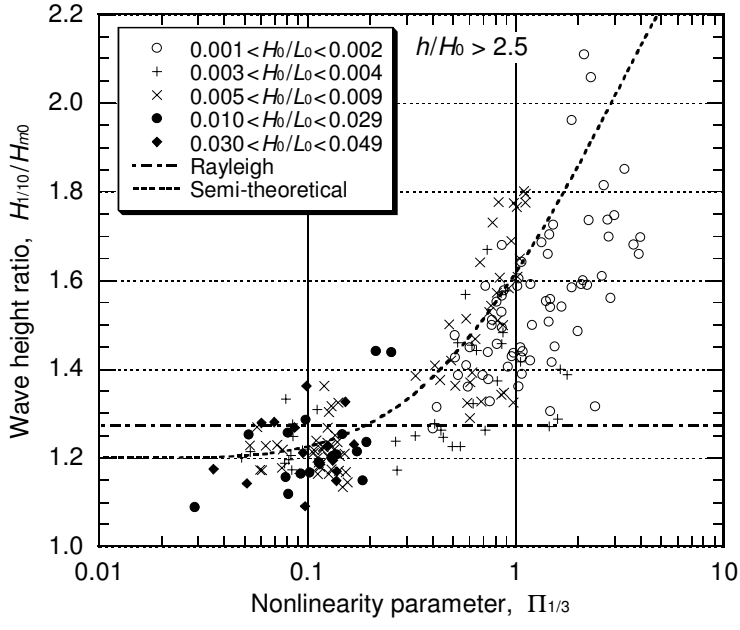

(a)

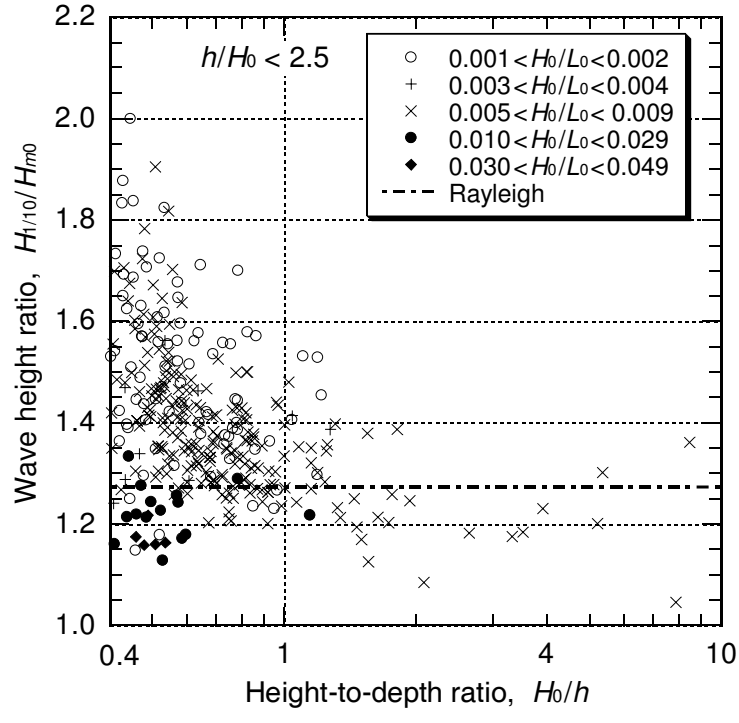

(b)

Fig. 11. Variation of wave height ratio $H_{1/10}/H_{m0}$ outside and inside the surf zone. (a) Outside the surf zone ($h/H_0 > 2.5$). (b) Inside the surf zone ($h/H_0 < 2.5$).

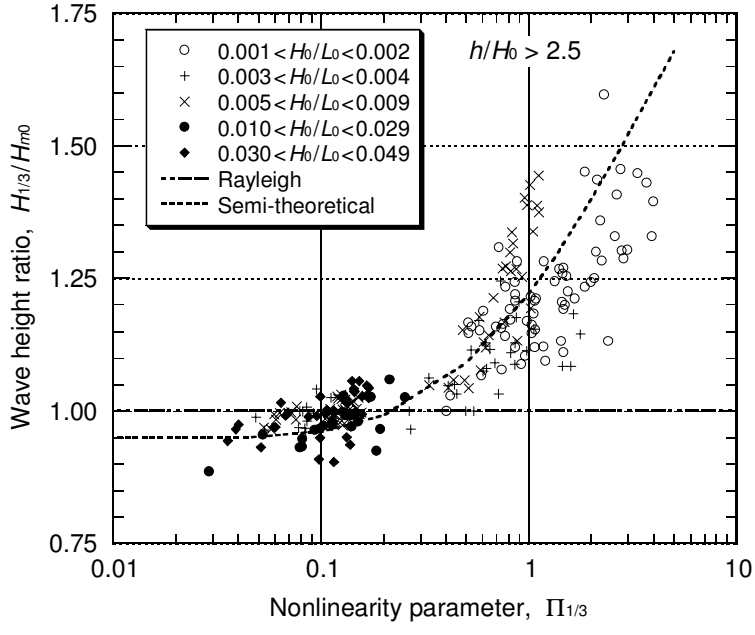

(a)

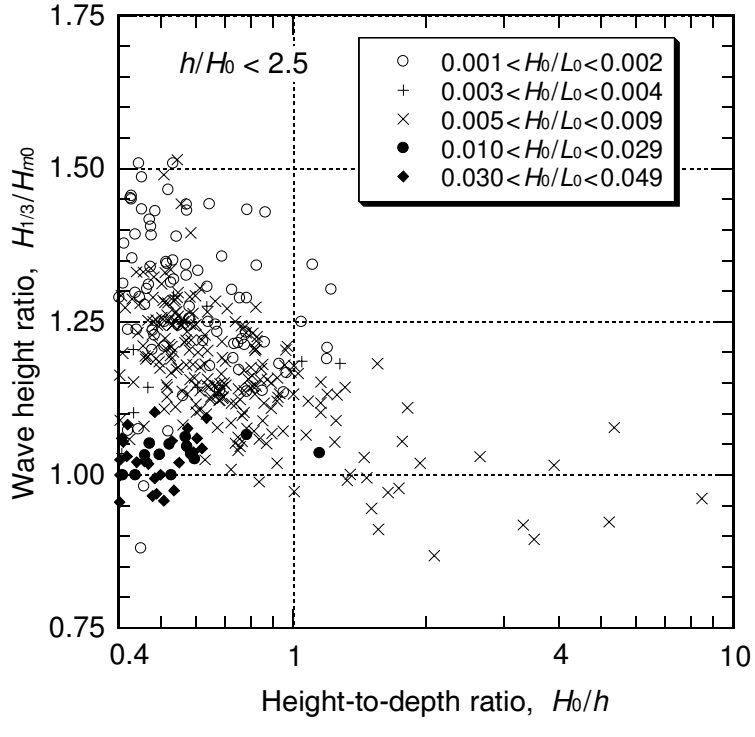

(b)

Fig. 12. Variation of wave height ratio $H_{1/3}/H_{m0}$ outside and inside the surf zone. (a) Outside the surf zone ($h/H_0 > 2.5$). (b) Inside the surf zone ($h/H_0 < 2.5$).

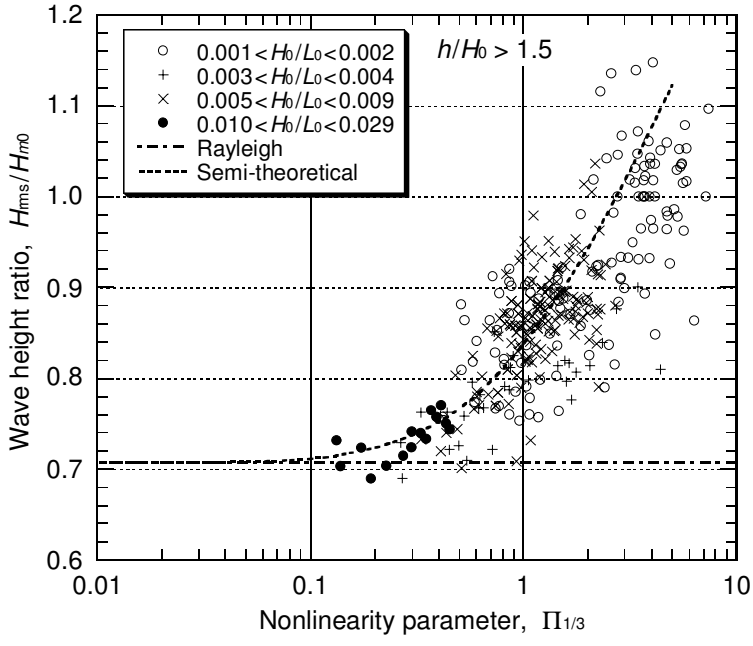

(a)

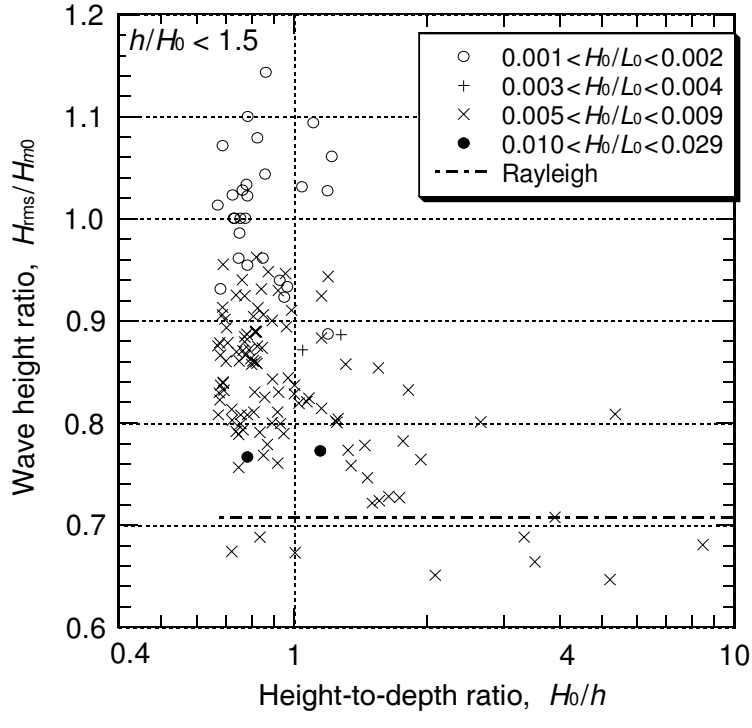

(b)

Fig. 13. Variation of wave height ratio $H_{\rm rms}/H_{m0}$ outside and inside the surf zone. (a) Outside the surf zone ($h/H_0 > 1.5$). (b) Inside the surf zone ($h/H_0 < 1.5$).

diagrams are for those outside the surf zone and the lower diagrams are for those inside the surf zone, same as those in Figs. 9 and 10. The boundary of the surf zone for $H_{1/10}$ and $H_{1/3}$ is subjectively set at $h/H_0 = 2.5$ in Figs. 11 and 12. In the case of the root-mean-square wave height $H_{\rm rms}$, the surf zone should be defined in a shallower area than for the significant wave, because $H_{\rm rms}$ is calculated with all individual waves. Thus, the boundary of $H_{\rm rms}$ was set at $h/H_0 = 1.5$ in Fig. 13.

The dashed lines in the upper diagrams are semi-theoretical predictions based on the potential energy calculation of finite amplitude waves and the Rayleigh distribution of wave heights, by referring to the methodology employed by Longuet-Higgins [1980]. Outside the surf zone shown in the upper diagrams of Figs. 11 to 13, the wave height ratios $H_{1/10}/H_{m0}$, $H_{1/3}/H_{m0}$, and $H_{\rm rms}/H_{m0}$ increase with the increase of the wave nonlinearity parameter. Although there is much scatter of data, they follow the trend of semi-theoretical curves. The one-tenth highest wave height $H_{1/10}$ in Fig. 11 is given the initial value of $1.20H_{m0}$ based on the trend of the data when considering the spectral shape effect.

The maximum values of the ratios of the statistical wave heights to the spectral significant wave height for swell of very low steepness are around 2.1 for $H_{1/10}/H_{m0}$, 1.6 for $H_{1/3}/H_{m0}$, and 1.15 for $H_{\rm rms}/H_{m0}$. With reference to the wave height ratios at the state of weak nonlinearity, the statistical wave heights are enhanced by 1.75 times for $H_{1/10}$, 1.68 times for $H_{1/3}$, and 1.64 times for $H_{\rm rms}$. Such enhancement of statistical wave heights are apparent ones without the real increase of wave energy as discussed before.

Such effects of wave steepness on the nonlinear features of waves inside the surf zone are originated from the fact that waves of low steepness experience a high degree of nonlinear wave shoaling before they are attenuated by breaking, while waves of high steepness are attenuated much earlier before they experience strong nonlinear shoaling. It is seen in the upper diagrams of Figs. 11 to 13 that waves with the steepness of 0.010 to 0.049 have the nonlinearity parameter up to $\Pi_{1/3} = 0.3$ only and waves are transferred into the lower diagrams which represent waves inside the surf zone. Waves with the steepness of 0.005 to 0.0099 have the nonlinearity parameter up to $\Pi_{1/3} = 1.2$ and moves into the group of those inside the surf zone. Waves with the steepness below 0.0029 can have the nonlinearity parameter up to $\Pi_{1/3} = 4$ before they enter into the surf zone.

Another way of depicting the wave nonlinearity effect on significant wave height is to use the following parameter Π_0 instead of $\Pi_{1/3}$:

$$\Pi_0 = \frac{H_0}{L_A} \coth^3 \frac{2\pi h}{L_A} \tag{16}$$

where the deepwater significant wave height H_0 is used in the numerator. The small amplitude wavelength L_A is calculated with the significant wave height $T_{1/3}$. Figure 14 is a re-plotting of the wave height ratio $H_{1/3}/H_{m0}$ against the nonlinearity parameter Π_0. The data shown in Fig. 12 was regrouped with a finer classification

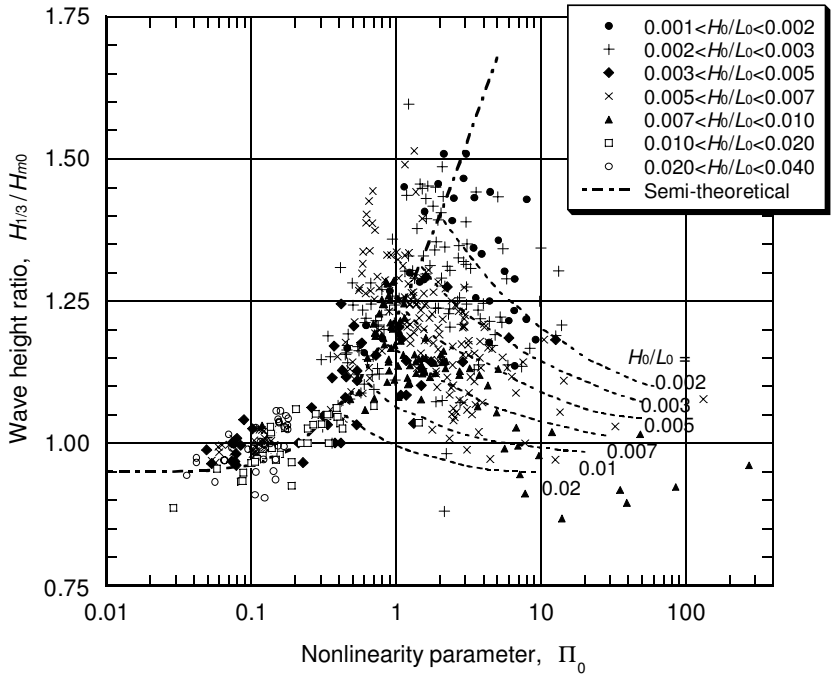

Fig. 14. Variation of wave height ratio $H_{1/3}/H_{m0}$ against wave nonlinearity parameter Π_0.

of wave steepness, and boundary lines between wave steepness groups were drawn subjectively to provide users with guide marks of wave height decrease in the surf zone. Figure 14 is equivalent to Fig. 6 of Thompson and Vincent [1985] (reproduced in Coastal Engineering Manual as Fig. II-1-40), though they did not provide actual data points and used different definitions of the abscissa and the wave steepness. The diagram of Fig. 14 will provide coastal engineers with a guideline to estimate nonlinear enhancement of zero-crossing significant wave height $H_{1/3}$ over the spectral significant height H_{m0}.

6. Conclusions

Wave breaking phenomenon in the nearshore waters are characterized by the following features:

(1) Breaker index or the ratio of breaker height to water depth is governed by both the beach slope and the relative water depth h_b/L_0.
(2) The breaker index formula by Goda [1975] for regular waves is revised by slightly reducing the beach slope effect for better agreement with laboratory data.
(3) Depth-limited breaker heights have inherent variability with the coefficient of variation of about 6% for the slope of zero to 1/50 and 14% for the slope of 1/10, which increases as the bed slope become steep.

(4) Incipient breaker index for the significant height of random waves is smaller than that for regular waves by about 30%, but the ratio of significant wave height to water depth gradually increases within the surf zone.
(5) Probability density function (*pdf*) of wave heights gradually deviates from the Rayleigh as waves propagate toward the shore, with the largest deviation taking place at the middle of the surf zone. However, the wave height distribution returns to the Rayleigh as waves approach the shoreline.
(6) Differences between characteristic wave heights such as $H_{2\%}$, $H_{1/10}$, $H_{1/3}$, and $H_{\rm rms}$ decrease in the middle of the surf zone, but they return to those by the Rayleigh near the shoreline. The PEGBIS model by Goda [2004] can simulate such changes of characteristic wave heights.
(7) Wave nonlinearity expressed in terms of skewness, kurtosis, and the wave ratios $H_{1/10}/H_{m0}$, $H_{1/3}/H_{m0}$, and $H_{\rm rms}/H_{m0}$ increases with wave propagation toward the shore, and it is most enhanced just outside of the surf zone. For swell of very low steepness, the skewness, kurtosis, and wave height ratio $H_{1/3}/H_{m0}$ may go up to 2.0, 9.0, and 1.6, respectively, at the wave nonlinearity parameter around 4.0.
(8) For wind waves and swell of relatively large steepness, random wave breaking begins at large depths compared with swell of small steepness. Thus, the former waves do not exhibit conspicuous wave nonlinearity.
(9) Wave nonlinearity is weakened by wave breaking inside the surf zone and is eventually lost near the shoreline with a return to linear wave features.

Acknowledgments

The author much appreciates kind cooperation by Dr. Steven Hughes and Dr. Shintaro Hotta for providing him with their valuable wave data of the photopole measurements. The author is also grateful to Dr. Luc Hamm for his PhD thesis and Danel's wave breaker data and to Dr. M.R.A. van Gent for $H_{2\%}$ data used in Fig. 7. The author further expresses his thanks to Dr. Bill Peirson for his valuable suggestions to improve the paper through his review work.

References

Battjes, J. A. [1972] "Setup due to irregular wave," in *Proc. 13th Int. Conf. Coastal Eng.*, Vancouver, *ASCE*, pp. 1993–2004.

Battjes, J. A. & Groenendijk, H. W. [2000] "Wave height distributions on shallow foreshores," *Coastal Engineering* **40**, 161–182.

Battjes, J. A. & Janssen, J. P. F. M. [1978] "Energy loss and set-up due to breaking of random waves," in *Proc. 16th Int. Conf. Coastal Eng.*, Hamburg, *ASCE*, pp. 1–19.

Black, K. P. & Rosenberg, M. A. [1992] "Semi-empirical treatment of wave transformation outside and inside the breaker line," *Coastal Engineering* **16**, 313–345.

Bowen, A. J., Inman, D. L. & Simmons, V. P. [1968] "Wave "set-down" and set-up," *J. Geophys. Res.* **73**(8), 2569–2576.

CIRIA; CUR; CETMEF [2007] *The Rock Manual. The Use of Rock in Hydraulic Engineering*, 2nd edition (CIRIA C683).

Danel, P. [1951] "On the limiting clapotis," *Gravity Waves, Proc. NBS Semicentennial Symp.*, June 1951, NBS Circular 521, pp. 35–38.

Ebersole, B. A. & Hughes, S. A. [1987] "DUCK85 photopole experiment," *US Army Corps of Engrs., WES, Misc. Paper*, CERC-87-18, pp. 1–165.

Galvin, C. J. Jr. [1969] "Breaker travel and choice of design wave height," *J. Waterways and Harbors Div., ASCE*, **95**(WW2), 175–200.

Goda, Y. [1964] "Wave forces on a vertical circular cylinder: Experiments and proposed method of wave force computation," *Rept. Port and Harbour Res. Inst.* **8**, 1–74.

Goda, Y. [1970] "A synthesis of breaker indices," *Trans. Japan Soc. Civil Engrs.* **2**(2), 39–49.

Goda, Y. [1973] "A new method of wave pressure calculation for the design of composite breakwaters," *Rept. Port and Harbour Res. Inst.* **14**(3), 59–106 (in Japanese).

Goda, Y. [1974] "New wave pressure formulae for composite breakwaters," in *Proc. 14th Int. Conf. Coastal Eng.*, Copenhagen, *ASCE*, pp. 1702–1720.

Goda, Y. [1975] "Deformation of irregular waves due to depth-controlled wave breaking," *Rept. Port and Harbour Res. Inst.* **12**(3), 31–69 (in Japanese) and "Irregular wave deformation in the surf zone," *Coastal Engineering in Japan, JSCE* **18**, 13–26.

Goda, Y. [1979] "A review on statistical interpretation of wave data," *Rept. Port and Harbour Res. Inst.* **18**(1), 5–32.

Goda, Y. [1983a] "Analysis of wave grouping and spectra of long-travelled swell," *Rept. Port and Harbour Res. Inst.* **22**(1), 3–41.

Goda, Y. [1983b] "A unified nonlinearity parameter of water waves," *Rept. Port and Harbour Res. Inst.* **22**(3), 3–30.

Goda, Y. [1988] "Statistical variability of sea state parameters as a function of wave spectrum," *Coastal Engineering in Japan* **31**(1), 39–52.

Goda, Y. [2000] *Random Seas and Design of Maritime Structures*, 2nd edition (World Scientific, Singapore).

Goda, Y. [2004] "A 2-D random wave transformation model with gradational breaker index," *Coastal Engineering Journal* **46**(1), 1–38.

Goda, Y. [2007] "How much do we know about wave breaking in the nearshore waters," in *Proc. 4th Int. Conf. Asian and Pacific Conf. (APAC 2007)*, CD-ROM, pp. 65–86.

Goda, Y. [2009] "A performance test of nearshore wave height prediction with CLASH datasets," *Coastal Engineering* **56**(3), 220–229.

Goda, Y., Haranaka, S. & Kitahata, M. [1966] "A study on impulsive breaking wave force upon a vertical pile," *Rept. Port and Harbour Res. Inst.* **5**(6), 1–30.

Goda, Y. & Kudaka, M. [2007] "On the role of spectral width and shape parameters in control of individual wave height distribution," *Coastal Engineering Journal* **49**(3), 311–335.

Goda, Y. & Nagai, K. [1974] "Investigation of the statistical properties of sea waves with field and simulation data," *Rept. Port and Harbour Res. Inst.* **13**(1), 3–37 (in Japanese).

Hamm, L. [1995] *Modelisation numerique didimensionnelle de la propagation de la houle dans la zone de deferlement*, Ph.D thesis, Universite Joseph Fourier.

Hamm, L. & Peronnard, C. [1997] "Wave parameters in the nearshore: A clarification," *Coastal Engineering* **32**, 119–135.

Hotta, S. & Mizuguchi, M. [1980] "A field study of waves in the surf zone," *Coastal Engineering in Japan, JSCE* **23**, 59–79.

Hotta, S. & Mizuguchi, M. [1986] "Statistical properties of field waves in the surf zone," in *Proc. 33rd Japanese Coastal Eng. Conf.*, pp. 154–157 (in Japanese).

ISO [2007] "ISO 21650 Actions from waves and currents on coastal structures," pp. 1–126.

Iversen, H. W. [1951] "Laboratory study of breakers," *Gravity Waves, Proc. NBS Semicentennial Symp.*, June 1951, NBS Circular 521, pp. 9–32.

Kaminsky, G. M. & Kraus, N. C. [1993] "Evaluation of depth-limited wave breaking criteria," in *Proc. 2nd Int. Symp. on Ocean Waves Measurement and Analysis, WAVES 1995*, pp. 180–193.

Kamphuis, J. W. [1991] "Incipient wave breaking," *Coastal Engineering* **15**, 185–203.
Kimura, A. & Seyama, A. [1986] "Breaking limit of irregular waves on slopes," in *Proc. 33rd Japanese Coastal Eng. Conf.*, pp. 174–178 (in Japanese).
Kishi, T. & Iohara, S. [1958] "Researches on coastal dikes (7) — experimental study on wave transformation and breaking waves —," *Rept. Public Works Res. Inst.* **95**, 185–197 (in Japanese).
Kriebel, D. [2000] "Breaking waves in intermediate-depths with and without current," *Coastal Engineering 2000 (Proc. Int. Conf.,* Sydney*), ASCE*, pp. 203–215.
Lara, J. L., Losada, I. J. & Liu, P. L.-F. [2006] "Breaking waves over a mild gravel slope: Experimental and numerical analysis," *J. Geophys. Res.* **111**(C11019), 1–26.
Li, Y. C., Dong, G. H. & Teng, B. [1991] "Wave breaker indices in finite water depth," *China Ocean Engineering* **5**(1), 51–64.
Li, Y. C., Yu, Y., Cui, L. F. & Dong, G. H. [2000a] "Experimental study of wave breaking on gentle slope," *China Ocean Engineering* **14**(1), 59–67.
Li, Y. C., Yu, Y., Cui, L. F. & Dong, G. H. [2000b] "Transformation and breaking of irregular waves on very gentle slope," *China Ocean Engineering* **14**(3), 261–278.
Longuet-Higgins, M. S. [1952] "On the statistical distributions of the heights of sea waves," *J. Marine Res.* **IX**(3), 245–266.
Longuet-Higgins, M. S. [1980] "On the distribution of the heights of sea waves: Some effects of nonlinearity and finite band effects," *J. Geophys. Res.* **85**(C3), 1519–1523.
McCowan, J. [1894] "On the highest waves in water," *Phil. Mag. Ser. 5* **36**, 351–358.
Miche, R. [1944] "Mouvements ondulatoires de lamer en profondeur ou décroissante," *Annles de Ponts et Chaussées* **19**, 370–406.
Mitsuyasu, H. [1962] "Experimental study on wave force against a wall," *Rept. Transportation Tech. Res. Inst.* **47**, 1–49.
Munk, W. H. [1949] "The solitary wave theory and its applications to surf problem," *Ann. New York Acad. Sci.* **51**, 376–423.
Muttray, M. & Oumeraci, H. [2000] "Wave transformation on the foreshore of coastal structure," *Coastal Engineering 2000* (*Proc. Int. Conf.,* Sydney)*, ASCE*, pp. 2178–2190.
Rattanapitikon, W. & Shibayama, T. [2000] "Verification and modification of breaker height formulas," *Coastal Engineering Journal* **42**(4), 389–406.
Rattanapitikon, W., Vivattanasirisak, T. & Shibayama, T. [2003] "A proposal of new breaker height formula," *Coastal Engineering Journal* **45**(1), 29–48.
Sallenger, A. H. & Holman, R. A. [1985] "Wave energy saturation on a natural beach of variable slope," *J. Geophys. Res.* **90**(C6), 11,939–11,944.
Seyama, A. & Kimura, A. [1988] "The measured propterties of irregular wave breaking and wave height change after breaking on the slope," in *Proc. 21st Int. Conf. Coastal Eng.*, Malaga, Spain, *ASCE*, pp. 419–497.
Smith, J. W. & Kraus, N. C. [1991] "Laboratory study of wave-breaking over bars and artificial reefs," *J. Waterway, Port, Coastal, and Ocean Eng., ASCE*, **117**(4), 307–325.
Smith, G., Wallast, I. & van Gent, M. R. A. [2002] "Rock slope stability with shallow foreshore," *Coastal Engineering 2002* (*Proc. Int. Conf.,* Cardiff, Wales)*, ASCE*, pp. 1524–1536.
Thompson, E. F. & Vincent, C. L. [1985] "Significant wave height for shallow water design," *J. Waterway, Port, Coastal, and Ocean Eng., ASCE* **111**(5), 828–841.
Ting, F. C. K. [2001] "Laboratory study of wave and turbulence velocities in a broad-banded irregular wave surf zone," *Coastal Engineering* **43**, 183–208.
Ting, F. C. K. [2002] "Laboratory study of wave and turbulence characteristics in a narrow-banded irregular breaking waves," *Coastal Engineering* **46**, 291–313.
Tominaga, M. & Hashimoto, H. [1972] "Run-up of irregular waves on a coastal dike," in *Proc. 19th Japanese Coastal Eng. Conf.*, pp. 303–307 (in Japanese).
Toyoshima, O., Tominaga, M. & Hashimoto, H. [1968] "Experimental study on wave transformation after breaking," *Rept. Public Works Res. Inst.* **133**, 121–129.

Yamada, H., Kimura, G. & Okabe, J. [1968] "Precise determination of the solitary waves of extreme height on water of a uniform depth," *Rep. Res. Inst. Applied Mech., Kyushu Univ.* **XVI**(52), 15–32.

Yamada, H. & Shiotani, T. [1968] "On the highest water waves of permanent type," *Bull. Disaster Prevention Res. Inst., Kyoto Univ.* **18-2**(135), 1–22.